SANDIA REPORT

SAND2013-2823
Unlimited Release
Printed January 2013

A Robust Approach to QMU, Validation, and Conservative Prediction

Daniel J. Segalman, Thomas L. Paez, Lara E. Bauman

Prepared by
Sandia National Laboratories
Albuquerque, New Mexico 87185 and Livermore, California 94550

Sandia National Laboratories is a multi-program laboratory managed and operated by Sandia Corporation, a wholly owned subsidiary of Lockheed Martin Corporation, for the U.S. Department of Energy's National Nuclear Security Administration under contract DE-AC04-94AL85000.

Issued by Sandia National Laboratories, operated for the United States Department of Energy by Sandia Corporation.

Available to DOE and DOE contractors from
U.S. Department of Energy
Office of Scientific and Technical Information
P.O. Box 62
Oak Ridge, TN 37831

Telephone: (865) 576-8401
Facsimile: (865) 576-5728
E-Mail: reports@adonis.osti.gov
Online ordering: http://www.osti.gov/bridge

Available to the public from
U.S. Department of Commerce
National Technical Information Service
5285 Port Royal Rd
Springfield, VA 22161

Telephone: (800) 553-6847
Facsimile: (703) 605-6900
E-Mail: orders@ntis.fedworld.gov
Online ordering: http://www.ntis.gov/help/ordermethods.asp?loc=7-4-0#online

SAND2013-2823
Unlimited Release
Printed January 2013

A Robust Approach to QMU, Validation, and Conservative Prediction

Daniel J. Segalman
Multi-Physics Modeling & Simulation Department
Sandia National Laboratories
Livermore, Ca 94550
djsegal@sandia.gov

Thomas L. Paez
Thomas Paez Consulting
185 Valley View Dr., Sedona, AZ, 86336
tlpaez4444@gmail.com

Lara E. Bauman
Quantitative Modeling & Analysis Department
Sandia National Laboratories
Livermore, Ca 94550
lebauma@sandia.gov

Abstract

A systematic approach to defining margin in a manner that incorporates statistical information and accommodates data uncertainty, but does not require assumptions about specific forms of the tails of distributions is developed. This approach extends to calculations underlying validation assessment and quantitatively conservative predictions.

Acknowledgment

The reviewers, Allen Robinson, Justin Newcomer, and James Lauffer, offered numerous suggestions that added greatly to the clarity of this report. We thank them.

We also thank our families for the patience that they showed as we spent what was nominally family time doing the work presented in this report.

Contents

Appendix

List of Figures

List of Tables

Nomenclature

$\text{ecdf}_{\{x_j\}}(x)$ The ECDF calculated from data sets $\{x_j\}$, page 27

CCDF Complementary Cumulative Distribution Function. CCDF = 1 - CDF, page 16

CDF Cumulative distribution function, page 16

DOF Degree of Freedom, page 14

ECDF Empirical cumulative distribution function, page 27

F_S Factor of Safety, page 15

F_X Cumulative distribution function of random variable X, page 16

f_X Probability density function of random variable X, page 16

F_Y Cumulative distribution function of random variable Y, page 16

f_Y Probability density function of random variable Y, page 16

KDE Kernel Density Estimator, page 28

L Load, or some analogous quantity, page 15

PDF Probability density Function, page 16

PEM Probability of exceeding margin, page 23

PoF Probability of failure, page 16

QMU Quantification of Margin and Uncertainty, page 21

RV Random Variable, page 15

S Strength, or some analogous quantity, page 15

X Random variable analogous to load, page 16

Y Random variable analogous to strength, page 16

This page intentionally left blank.

Chapter 1

Introduction

It is an unfortunate irony of life that

1. The less reliable a design is, the easier it is to make meaningful estimates for probability of failure.

2. The more reliable it is, the less meaningful are efforts to quantify that reliability.

Quite naturally, the more reliable the system is, the more natural it is to discuss that reliability in terms of *margin*. Even margin must be discussed in a probabilistic sense. Added to this conceptual complexity is the necessity of quantifying our confidence in the margins and probabilities that we discuss.

The focus of this monograph is to introduce a formalism in which margin, probability and confidence all fit together quite naturally. Additionally, the necessary computations are intuitive and reasonably easy to perform.

The approach presented here is "minimalist" in the sense that it involves minimal dependence on components that are not well known, such as the precise form of the relevant distributions or the content of the tails of those distributions. This is consistent with the use of the term in design: using the fewest and barest essentials or elements for a maximal effect. As will be seen below, it is also constructed to be robust.

Outline of Presentation

The order of this narrative is as follows.

1. Some of the limitations of common approaches to defining margin as well as the difficulties in connecting margin with probability of failure are discussed here in the introduction.

2. A new concept for defining margin is presented in Chapter 2. This is a concept which clearly connects the definition of margin with the calculation of probability of failure. This new concept, Probability of Exceeding Margin (PEM), minimizes sensitivity of failure probability estimates to tail shapes in load and strength probability distributions.

3. Use of re-sampling in calculating confidence values of PEM is demonstrated in Chapter 3.

4. The concept of PEM could be employed in various manners to define validation criteria. One very natural approach to this is demonstrated in Chapter 4.

5. A theorem of set theory is employed in Chapter 5 to use PEM along with the sort of statistical information employed in model validation to overcome accuracy limitations of models to make confidently conservative predictions.

6. Discussion and conclusion.

A Simple Illustration

To introduce our new approach, we begin with a re-examination of the standard reliability calculation. Consider the structure shown in Figure 1.1. It is base-driven, has 30 discrete masses,

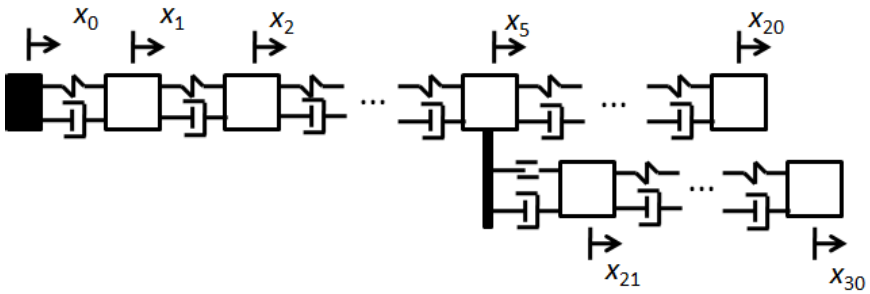

Figure 1.1: An otherwise linear structure with nonlinear elements between nodes 5 and 21.

and responds in one dimension. The quantities x_j, $j = 0,\ldots,30$ denote absolute displacements of the base and the system masses; these also denote degrees-of-freedom (DOF) of the structure. The mass of the element under x_0 is immaterial to the analysis; the mass is rigid and a motion is enforced at that location. The elements associated with the displacements x_j, $j = 1,\ldots,30$, have masses m_j, $j = 1,\ldots,30$. The damper to the left of DOF j is denoted c_j, $j = 1,\ldots,30$. The spring to the left of DOF j (except for DOF 21) is denoted k_j, $j = 1,\ldots,30$. The spring to the left of DOF 21 is nonlinear, and the restoring force in that spring is denoted $R(x_{21} - x_5)$. The element shown as solid black that extends down from DOF 5 is a rigid, massless element. The parameters of various

elements of this structure must be treated as random variables. This system is described in detail in Appendix E.

At this stage, for the sake of discussion we shall assume that there are numerous nominal acceleration histories whose application on the base of the structure is anticipated. Because of uncertainty in the base acceleration and because of the partially random character of the structure, the peak load anticipated at the location of a sensitive component at location 26 must be treated as a Random Variable (RV) L (for *Load*). For the sake of illustration, we shall assume that 30 realizations have been achieved (either through test or simulation). Additionally, failure loads of the component at location 26 are also known in a statistical sense. We refer to this random variable as *Strength* S. We shall assume that we have 25 realizations of S.

Properly normalized (integrate to 1) histograms of both L and S realizations are shown in Figure 1.2. Define Factor of Safety, F_S by

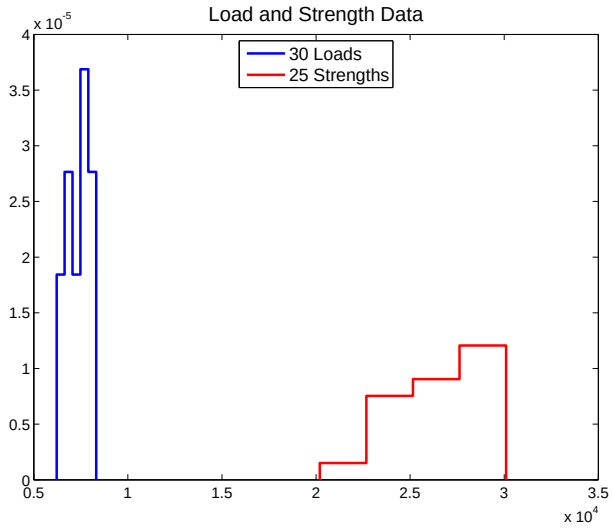

Figure 1.2: Histogram of 30 loads and 25 strengths. The histograms are each normalized to integrate to one.

$$F_S = \text{Estimate of minimum}(S)/\text{Estimate of maximum}(L). \tag{1.1}$$

Examination of these histograms would on several bases suggest that the design is very safe. Division of the lowest strength (2.02e+04) by the highest load (8.14e+03) yields a comforting Factor of Safety (F_S) of 2.5. Because

$$\text{Margin} = \text{Estimate of minimum}(S) - \text{Estimate of maximum}(L) \tag{1.2}$$

we see that F_S is another way of expressing Margin. Of course, had we more data, we might expect that our minimum realization of S would decrease and that our maximum realization of L would

increase, resulting in a much less optimistic estimate for factor of safety. This can be a serious difficulty, but it is addressed by recasting the problem probabilistically.

This is done through estimation of the Probability of Failure (PoF). From this point on, we acknowledge that neither load nor strength can be so well known that they can be considered deterministic quantities. We now refer to load and strength as random variables X and Y, respectively. A straight-forward estimate of the probability of failure (assuming statistical independence of load and strength) would integrate the joint probability density function (PDF) of load and strength over the region where load is greater than strength:

$$P_F = \int_{x>y} f_X(x)\, f_Y(y)\, dx\, dy = \int_{-\infty}^{\infty} f_Y(y) \left(\int_{y}^{\infty} f_X(x) dx \right) dy$$

$$= \int_{-\infty}^{\infty} f_Y(y) \left[1 - F_X(y) \right] dy \tag{1.3}$$

where $f_X(x)$ is the PDF of load, $F_Y(y)$ is the cumulative distribution function (CDF) of strength. The quantity in brackets in Equation 1.3 $[1 - F_X(y)]$ is referred to as the *complementary* cumulative distribution function (CCDF).

(Above, we have assumed that random variable X representing load and the random variable Y representing strength are independent of each other. This is generally a very reasonable assumption, and where it does not hold, an extended version of the following development can be made for such cases as well.)

Were we to employ the normalized histograms of Figure 1.2 for f_X and f_Y our estimate for the probability of failure for our system would be exactly zero; there are no loads larger than our lowest strength. This is clearly wrong. This approach suffers from the same limitation as does our estimate for the Factor of Safety above; more data could substantially change our estimate for PoF.

For the above reason, it is standard practice to postulate a form for the PDF for load, to postulate a form for the PDF of strength, to fit those distributions to the available data by some method (maximum likelihood is used in the following), and then to perform the necessary integrations. For instance, a typical problem might involve a sampling of applied loads that might be seen by a component and a sampling of strengths associated with such components. (Load and Strength are used as proxies for analogous quantities that would arise in other sorts of analysis - such as electrical, optical, or even financial systems.) A common practice is for the analyst 1) to assert that each of these sample sets conforms to some standard distribution [1] [2], 2) to estimate the distribution parameters to match the available data, and 3) to employ those fitted distributions to perform reliability estimation, while setting aside the original data.

As an exercise, three common distributions (normal, log-normal, and generalized extreme

[1] Often Gaussian, chi-square, exponential, generalized extreme value [13], log-normal, etc.

[2] The reader may find some footnotes helpful, but the reader could ignore all footnotes without serious loss.

value) were fit to each of the load and strength data using Matlab®'s maximum likelihood functions. These distributions are defined in Appendix A; they were chosen for their tendencies to emphasize or to de-emphasize tails. Plots of those distributions are shown in Figure 1.3.

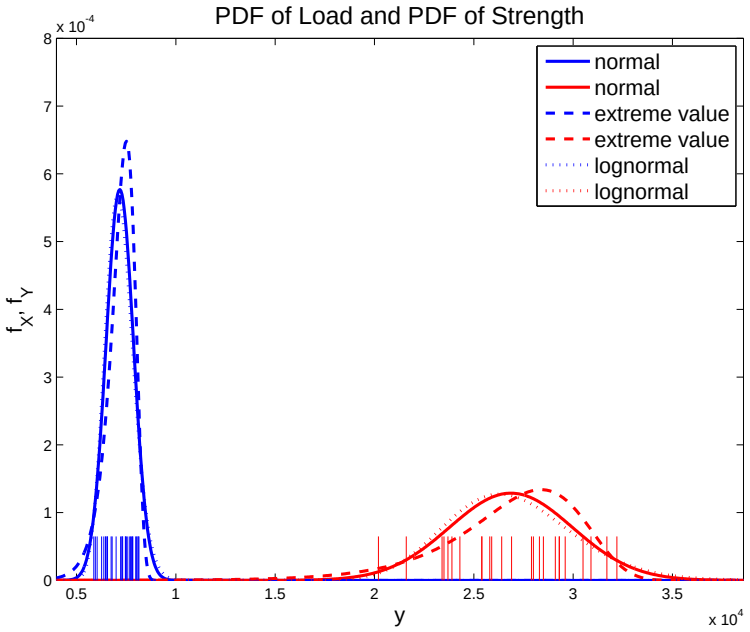

Figure 1.3: Multiple distributions fitted to the available load and strength realizations. The load and strength data are indicated by blue and red tick marks, respectively.

One sees that those distributions look similar in the regions where the data is clustered[3]. On the other hand, we know that the asymptotic behaviors of those distributions are quite different for large arguments [6]. This is borne out by calculation of PoF for each combination of distributions of load and strength shown in Table 1.1.

Load	Strength	PoF
extreme value	lognormal	3.7e-24
normal	lognormal	1.2e-20
lognormal	lognormal	5.8e-18
extreme value	normal	2.3e-10
normal	normal	2.8e-10
lognormal	normal	3.5e-10
normal	extreme value	4.2e-04
extreme value	extreme value	4.2e-04
lognormal	extreme value	4.2e-04

Table 1.1: Predicted PoF for 30 loads and 25 strengths.

In Table 1.1 we see ten's of orders of magnitude difference among the calculated PoFs. This is a fundamental problem: by postulating a PDF for load or strength, we are effectively extrapolating the character of the distribution of those quantities far beyond the region where we actually have data. One might assert that the problem goes away if one were to choose the "right" distribution form, but generally an adequate distribution form cannot be known a priori. Additionally, as Weibull points out [23], one cannot expect there to exist a "right" distribution form [4].

From the above, we see that

1. Consideration of margin alone is inadequate; margin may change substantially as new data becomes available.

2. Consideration of PDF alone is also inadequate; what PoF one obtains by evaluation of Equation 1.3 may depend dramatically on the forms of PDF postulated for loads and for strengths.

What is needed is an approach to merge PoF and margin in a manner that provides useful information, but that is also reasonably insensitive to the addition of small amounts of new data and that does not require extrapolation with respect to the tails of the PDFs.

[3]None of the PDF forms used to fit the load data failed the Kolmogorov-Smirnov goodness-of-fit test at 5% significance and none of the PDF forms used to fit the strength data failed that test. See [2] for a discussion on goodness-of-fit testing.

[4]Weibull's observation is "The objection has been stated that this distribution function has no theoretical basis. But in so far as the author understands, there are-with very few exceptions-the same objections against all other df, applied to real populations from natural or biological fields, at least in so far as the theoretical basis has anything to do with the population in question."

An Exploration

Suppose that we did not have the distribution of load data shown in the blue histogram in Figure 1.2. Instead we consider several other hypothetical distributions of load; each distribution has shape identical to the original blue histogram, but is offset from the original blue histogram by an amount M, where M is different for each distribution considered. For each of those values of M and the corresponding load distributions, we again fit several distributions and calculate probability of failure.

The calculated PoFs that result are shown in Figure 1.4. At each value of M, there are nine different computed probabilities of failure. Each corresponds to the calculation as though the load data of Figure 1.2 were shifted to the right by an amount M. The new load data and the strength data were each fitted by the PDF forms indicated in the legend, and Equation 1.3 was employed to calculate the probability of failure.

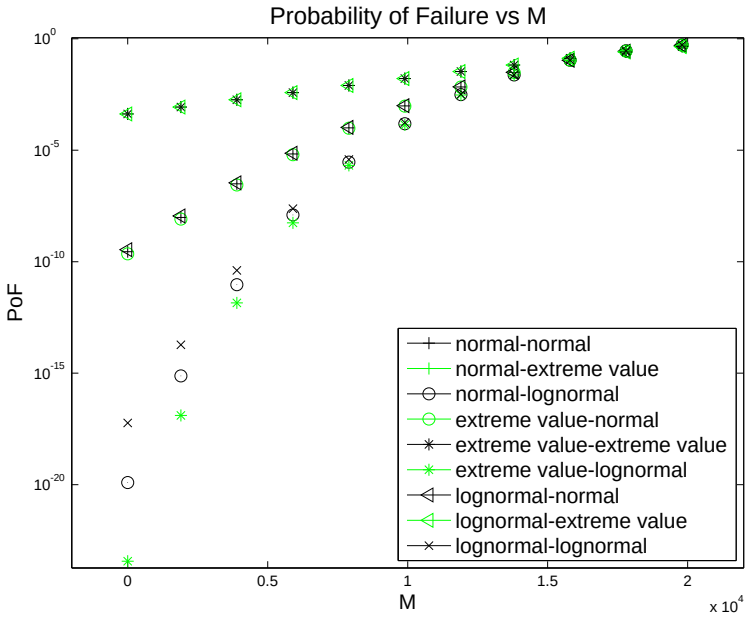

Figure 1.4: Probability of Failure (PoF) calculated using multiple distributions fitted to the shifted load and strength data.

One sees that the orders of magnitude differences in predicted PoF begin to disappear as the distributions of load realizations approach those of strength. Where we choose to say that the upper and lower estimates for PoF converge is fairly arbitrary. Examining Figure 1.4, we see that at about a value of $M = 15200$, the maximum estimate for PoF is within 50% of the minimum estimate. Let's call that value M_{50}. Alternatively, we could consider $M_{95/5}$ at which the top 5% of loads extend beyond the bottom 5% of strengths. In this case, $M_{95/5} = 13500$. The translation that results in that overlap is illustrated notionally in Figure 1.5.

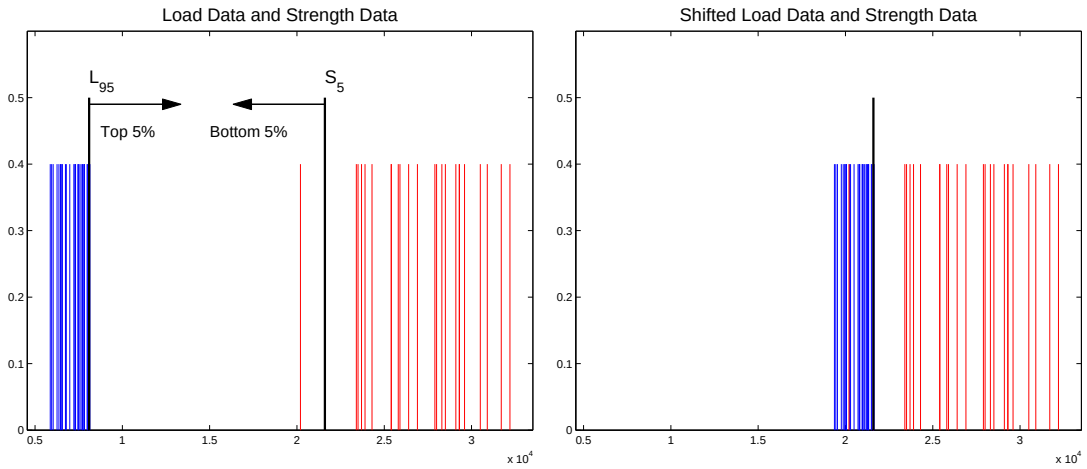

Figure 1.5: A notional depiction of the translation of load realizations that causes the top 5 % of the revised load to extend beyond the bottom 5 % of the strengths.

In our numerical explorations, the translation M_{50} that narrows the span of PoFs to within 50% is generally very close to the translation $M_{95/5}$ discussed above. The load realizations translated by $M_{95/5}$ and the approximating load PDFs, along with the strength realizations and the approximating strength PDFs are shown in Figure 1.6.

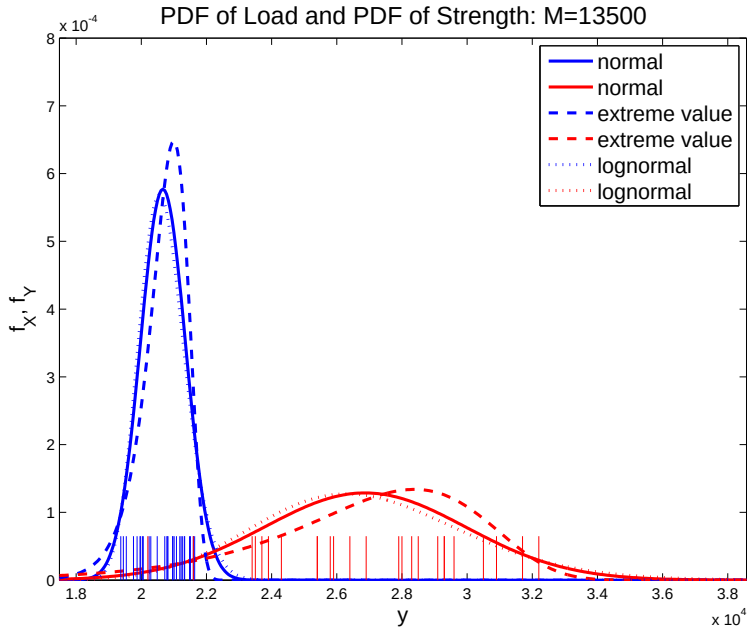

Figure 1.6: The load realizations translated by $M_{95/5}$, their approximating PDFs, the strength realizations, and their approximate strength PDFs.

The calculated PoFs for the problem when the loads are translated by $M_{95/5}$ are shown in Table 1.2. In this table, we see, as expected, that for this hypothetical problem, the calculated probabilities of failure are reasonably independent of the postulated forms of the load and strength PDFs.

Load	Strength	PoF
extreme value	lognormal	1.8e-02
normal	lognormal	1.9e-02
lognormal	lognormal	1.9e-02
extreme value	normal	2.5e-02
normal	normal	2.5e-02
lognormal	normal	2.6e-02
normal	extreme value	6.0e-02
extreme value	extreme value	6.0e-02
lognormal	extreme value	6.0e-02

Table 1.2: Predicted PoF for 30 loads and 25 strengths and $M = M_{95/5} = 13500$.

If it were always the case that the design were so unconservative that a $95/5$ overlap of load and strength data could be counted on, one would then always expect to obtain a (reasonably) unambiguous estimate for probability of failure.

Comments on Nomenclature

This would appear to be an appropriate place to connect the problem and language of this chapter to that most conventional in the Quantification of Margin and Uncertainty (QMU) community. The conclusions drawn from the above example could as easily apply to almost any unidirectional QMU problem via the following:

1. Where load and strength occurred in the above discussion, one could as easily consider any other performance and threshold variables, respectively. (In the following we continue to use terms "load" and "strength" for the purpose of continuity.
2. In this problem, both the performance and threshold variables (as is the most general case) and our knowledge of them is represented by cumulative distribution functions. It often happens that our knowledge of one or the other of these random variables is so thin that we represent the character of that variable with a single "cut off" value and the CDF is a Heaviside function that switches on at that value. The mathematical arguments presented above and below hold as well in this case as they do in the case where the characters of both random variables are represented by more continuous CDFs.

This page intentionally left blank.

Chapter 2

Probability of Exceeding Margin (PEM)

As one might have anticipated from the previous section, we introduce the notions of *Margin* and *Probability of Failure* in an integrated manner.

The Concept

Let us define the **minimum margin** $M_{\min}$ of a problem involving load realizations $\{x_j\}$ and strength realizations $\{y_k\}$ to be the minimum value M such that the calculated probability of failure of the load plus $M_{\min}$ can be calculated with confidence (without dependence on the tails of presumed PDFs). For every margin $M > M_{\min}$ we have a corresponding probability of failure $P_F(M)$.

The $95/5$ **margin** $M_{95/5}$ was defined in the previous section to be the number $M_{95/5}$ that when added to each member of the set of load realizations will cause an overlap of the top 5% of the loads with the bottom 5% of the strengths. It has been the authors' experience that $M_{95/5}$ is a reasonable approximation for $M_{\min}$. In the absence of numerical experiments to establish $M_{\min}$ we may just approximate it by $M_{95/5}$:

$$M_{\min} \approx M_{95/5} \tag{2.1}$$

The key concept is that statements about a system's reliability must involve both a margin $M > M_{\min}$ and the corresponding probability of failure, calculated using available load and strength realizations and margin M:

$$P_F(M) = \int_{x+M>y} f_X(x)\, f_Y(y)\, dx\, dy = \int_{-\infty}^{\infty} f_Y(y) \left(\int_{y-M}^{\infty} f_X(x) dx \right) dy$$

$$= \int_{-\infty}^{\infty} f_Y(y) \big(1 - F_X(y-M)\big)\, dy \tag{2.2}$$

where $f_X(x)$ and $F_X(x)$ are as defined after Equation 1.3.

The sense of this integral can be understood either through the translation indicated in Figure 1.5 or by examination of Figure 2.1.

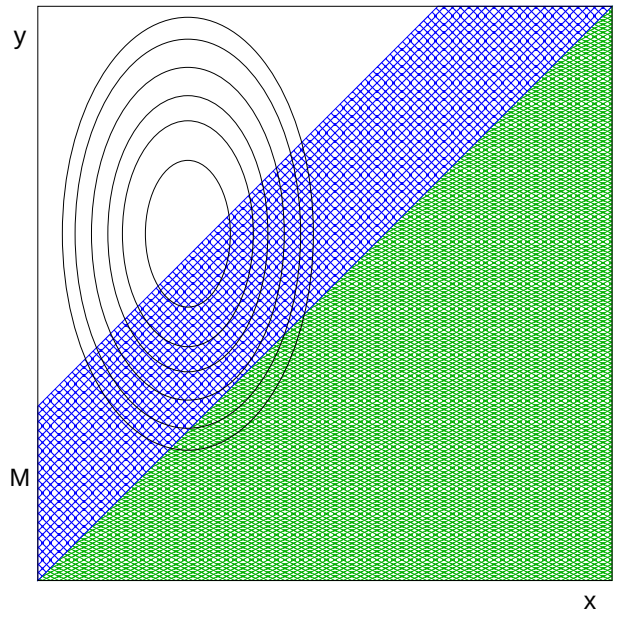

Figure 2.1: Contours of the joint PDF, $f_X\, f_Y$ (ellipsoids) and integration domains of Equations 1.3 (lower, green cross-hatched region) and 2.2 (blue and green cross-hatched regions).

In that figure, contours of the product of f_X and f_Y are laid out; the region where $X > Y$ is shaded green. Almost all of the green area lies in a region of very tiny probability, and only slightly overlaps the outer edge of the outermost contour. The region where $X + M > Y$ is shown in blue. It completely covers the green region and also covers almost half of the contour plot. Let's consider the volume sandwiched by the x and y plane and the $f_X f_Y$ surface. By shifting by margin M, we are no longer trying to evaluate a region with very little of that volume, instead we now evaluate over a good fraction of that volume. Even if very little of the integrand $f_X Y$ lies within the first region, the quantity M can be made large enough so that the blue region covers a substantial part of the integrand. A formal proof of this is given in Appendix B.

Making Statements

Statistical Statements

In the problem considered here, one could use the above calculations to make statements such as

The probability that the load plus 13500 exceeds strength is on the order of 3.5%.

No assumption of the form of PDF for either Load or Strength is necessary to make the above statement. Such statements can be made with some confidence because by integrating margin into the probabilistic statement, we have removed any strong dependence on the tails of the distributions that underlie our available realizations. (See figure 2.1 for an illustration of the concept or see the proof in Appendix B).

To illustrate this relative independence from the tails, most of the examples below are presented with two very different sorts of distribution: one with a common (Gaussian) tail and one with no tail at all.

Engineering Statements

A statement involving 3.5% probability of failure will not make any system engineer comfortable. It must be emphasized that we are not actually talking about a real probability of failure, but rather we are discussing a 3.5% probability of load plus margin exceeding strength. More succinctly we now speak in terms of *Probability of Exceeding Margin* or **PEM** as defined by the probability of failure integral (2.2) which we repeat here.

$$PEM = P_F(M) = \int_{-\infty}^{\infty} f_Y(y)\big(1 - F_X(y-M)\big)\,dy \tag{2.3}$$

where $f_X(x)$ and $F_X(x)$ are as defined after Equation 1.3.

The rest of the story depends on the engineers. The statisticians provide the probabilistically derived margin $M = M_{95/5}$. It is the job of the engineers to provide physics-based arguments as to why this margin M is conservative. For instance, the engineers might find physically motivated arguments for a lower bound for margin that is larger than the statistically derived margin introduced above.

More Considerations

1. One could as easily consider a different distribution of strength: $Y_M = Y - M$. The calculations for probability of load plus margin exceeding strength (PEM) are analogous to those done above and the results are numerically identical.

2. In practice, one would consider a margin M_L for load and a margin M_S for strength such that one could argue that both M_L and M_S are sufficiently conservative and one would perform the calculations of the previous section employing margin $M = M_L + M_S$. Use of M_L and M_S together evokes the original ideas used to define Quantification of Margins and Uncertainties (QMU)[17].

Prospective and Retrospective Margins

The use here of the concept of *margin* is retrospective in nature. It is calculated once a design candidate has been identified and appropriate testing of simulation is performed. Margin is also commonly used in another sense in which the margin is employed as a design goal and the designer chooses a strategy to meet or exceed that goal.

The term "factor-of-safety" is also used in similar prospective and retrospective senses. In aerospace a factor of safety of 1.5 is the standard design goal, though retrospective test/analysis generally yield larger values.

Implementation without Tails

The key notion above was the definition of margin so that the calculated probability of load plus margin exceeding strength would be reasonably independent of the forms of distribution assumed. In this section we demonstrate this approach in a manner where the assumed distribution forms have *no* tails. As a point of this formulation is to provide reliability estimates without extrapolation beyond the existent data, it is only natural to employ in this example distributions whose support is restricted to the regions where data exist.

For this purpose we approximate

$$f_X(x) \approx \frac{1}{N_x} \sum_j \delta(x - x_j) \tag{2.4}$$

where N_x is the number of realizations of load data, $\{x_j\}$ are those data values, and δ is the Dirac delta function. Similarly

$$f_Y(y) \approx \frac{1}{N_y} \sum_k \delta(y - y_k) \tag{2.5}$$

where N_y is the number of realizations of load data and $\{y_k\}$ are those data values.

The cumulative distributions for load and strength become

$$F_X(x) \approx \frac{1}{N_x} \sum_k H(x - x_k) \tag{2.6}$$

and

$$F_Y(y) \approx \frac{1}{N_y} \sum_k H(y - y_k) \tag{2.7}$$

where $H()$ is the Heaviside function. The above are exactly the empirical cumulative distribution functions for X and Y, respectively (ECDF)[1], which we more concisely write as

$$F_X(x) \approx \text{ecdf}_{\{x_j\}}(x) \quad \text{and} \quad F_Y(y) \approx \text{ecdf}_{\{y_j\}}(y) \tag{2.8}$$

Substituting approximations 2.4 and 2.8 into Equation 2.3

$$P_F(M) = \frac{1}{N_x}\sum_k \left[1 - \text{ecdf}_{\{x_j\}}(y_k - M)\right] = 1 - \frac{1}{N_x}\sum_k \text{ecdf}_{\{x_j\}}(y_k - M) \tag{2.9}$$

The above expression is interesting; it shows that for this tailless representation for load and strength distributions, the PEM is expressed as a sum of the complementary empirical cumulative distribution function evaluated at points $y_k - M$. The ingredients of this calculation for our example problem are shown in Figure 2.2. This calculation yields an estimate for probability of exceeding margin of 3.1%, not too distant from mean value (3.5%) over all distribution forms discussed earlier.

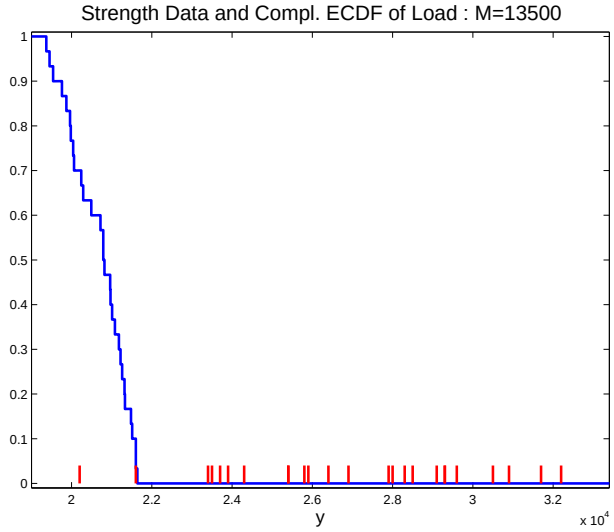

Figure 2.2: The PEM can be approximated using a combination of the empirical cumulative distribution function of load and a delta function approximation for the PDF of strength.

[1]The empirical cumulative distribution function is an stair-step estimate for the CDF of an underlying distribution created by incrementing by $1/n$ at the location of each data point.

Illustration Using Kernel Density Estimators

In the previous section, discrete functions were used to represent the relevant distributions and to calculate the relevant integrals in Equation 2.3. In this procedure, no probability is assigned outside the interval where data is observed. Some will assert that eliminating hypothetical data from the statistical analysis is the best approach. Others may insist that statistical analysis must include distributions with tails, admitting the possibility of some events occurring outside the observed interval.

Kernel Density Estimators (KDE) provide a way to allow tails but still concentrate the probability mass on the observed data [21, 20]. Though the implementation of the necessary numerical integration is a bit more complicated than that employed in the earlier sections, it is worthwhile to illustrate KDE in the context of the QMU approach of this monograph. (KDE is discussed briefly in the box at the end of this chapter, but its details are unimportant to the demonstration presented here.)

Considering the same load and strength data employed above, the KDE estimates for the complementary CDF for load and for the PDF for the strength are shown in Figure 2.3. Using these approximations in equation 2.3 to yield an estimate for probability of exceeding margin of 4.9%. For comparison, the mean probability of failure over many distributions with tails is (3.5%). The PEM calculated with discrete approximations is 3.1%. These results illustrate clearly how the PEM approach produces estimates with minimal dependence on the forms of distribution employed. We have similar estimates 1) for distributions (KDE) where the assumed distribution form entailed a significant tail 2) where we average over a number of distributional forms and 3) for distributions that involve NO tail.

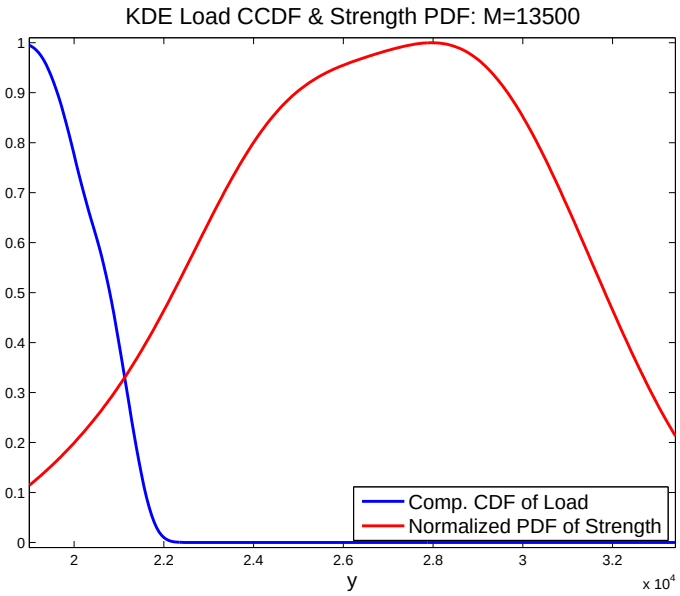

Figure 2.3: The PEM can be estimated by integrating the product of the KDE approximations for the PDF (f_Y) for strength and the complementary CDF for translated load ($1 - F_X(x - M)$). To put both plots in the same figure, the PDF of strength is normalized by its peak value.

About KDE Approximation

A Kernel Density Estimator [21, 20]. for a PDF on the basis of a finite set of data is an expression of the form

$$f_X(x) \approx \frac{1}{h_X N_x} \sum_j K\left(\frac{x - x_j}{h_X}\right) \tag{2.10}$$

where K is the kernel, a non-negative function of its argument such that $\int_{-\infty}^{\infty} K(s)ds = 1$ (a probability distribution) and h_X is an appropriately chosen characteristic length. N_x are the number of data points x and $\{x_j\}$ are the values of these data points.

Among the more popular kernel functions K used in KDE is the normal distribution. When a normal distribution is used as the kernel function, the characteristic length h_x is commonly chosen to be a function of the observed standard deviation $\hat{\sigma}_X$, that is, $h_X = 1.06\hat{\sigma}_X(1/N_x)^{-1/5}$. As an illustration using four data points, Figure 2.4 shows the KDE estimate of PDF (black curve) as well as the contribution of each data point to the final estimate of the distribution (colored curves).

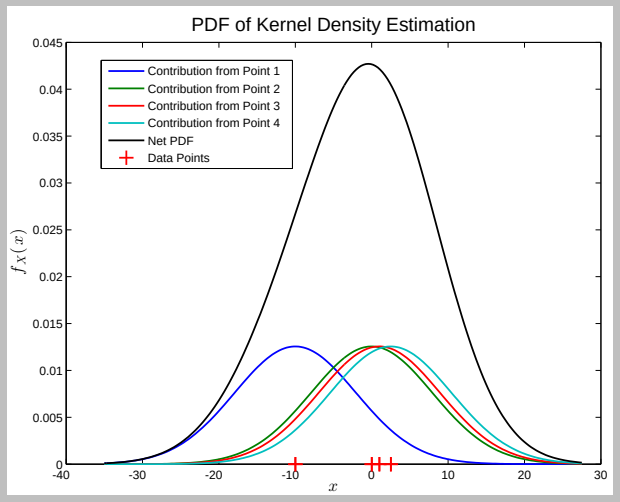

Figure 2.4: PFD constructed from a handful of discrete points using Kernel Density Estimation (KDE) and a reference Gaussian distribution.

Chapter 3

Calculation of Confidence

As is usually the case when making probabilistic statements, one must also make some estimate for confidence in those probabilistic statements. Thus far, we have avoided parameterized distributions and seek a confidence estimator that is also non-parameterized. Re-sampling techniques provide such a strategy, and we illustrate the development of confidence values for the quantification of margin using the bootstrapping re-sampling technique [10], [9]. Such techniques involve generation of a multiplicity of artificial sample sets and the estimation of confidence in parameters of the distribution from which the samples were drawn. Resampling techniques have validity in estimating features of the underlying distribution only with respect to features comfortably within the range of the sample set, and this meshes nicely with the PEM approach.

There is a short discussion on bootstrapping in a box at the end of this chapter (which the reader may skip without engendering significant discontinuity in the presentation) and there is a chapter on the subject in Appendix D (which the interested reader will find very accessible.)

Confidence Estimation Employing Discrete Distributions

The bootstrap technique is used to generate $B = 1000$ replicates of the PEM as follows (steps 1 and 2 discussed in the box). For each load replicate and for each strength replicate, an empirical cumulative distribution function (ECDF, Equation 2.6) was calculated. The bootstrap replicates of the load ECDF are shown in the left graph of Figure 3.1. This is a visual demonstration of the sampling distribution of the ECDF. The thick, jagged blue curve indicates the 20 *percentile* of the ensemble of load distributions. The bootstrap replicates of strength are plotted in ECDF form in the right graph of Figure 3.1. The thick, red curve in the figure indicates the 80 *percentile* of the ensemble of strength distributions.

These 1000 ECDFs of shifted load and an equal number of PDFs of strength were used to generate 1000 estimates of PEM (Equation 2.9.) These estimates are sorted in ascending order and the $(1-\alpha)\times 100$ *percent* upper limit of the PEM was identified. Our analysis used $\alpha = 0.2$ and $M = 13500$ to obtain an 80 *percent* confidence that $P_F\left(X + 13500 > Y\right) \leq 0.093$

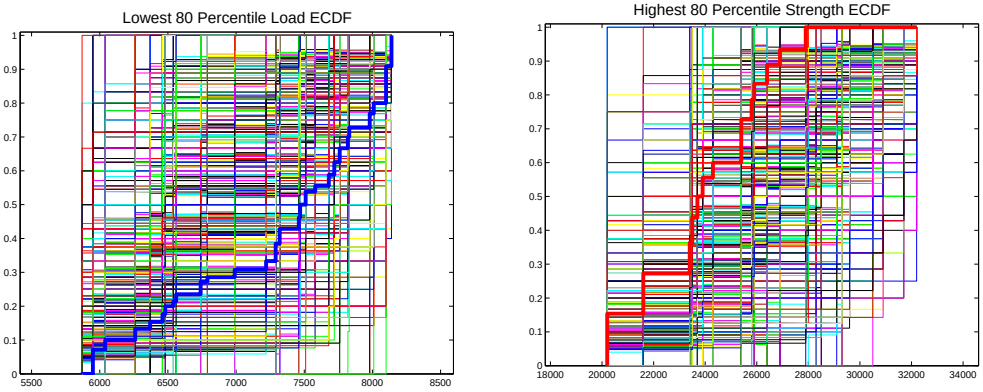

Figure 3.1: Bootstrap re-sampling is used to obtain 1000 other plausible sets of realizations of load and of strength. The low 20% load and the high 20% strength distributions are shown in thick blue and red lines, respectively.

Confidence Estimation Employing KDE

To demonstrate a reasonable independence from the form of distribution employed, we repeat the above analysis using KDE to represent the PDF of random strengths and the integral of KDE to represent the CDF of random loads. (Plots of the bootstrapped KDE representations for load and strength CDFs are shown in Figure 3.2. The solid blue and red curves have the same meanings in this figure as in Figure 3.1.)

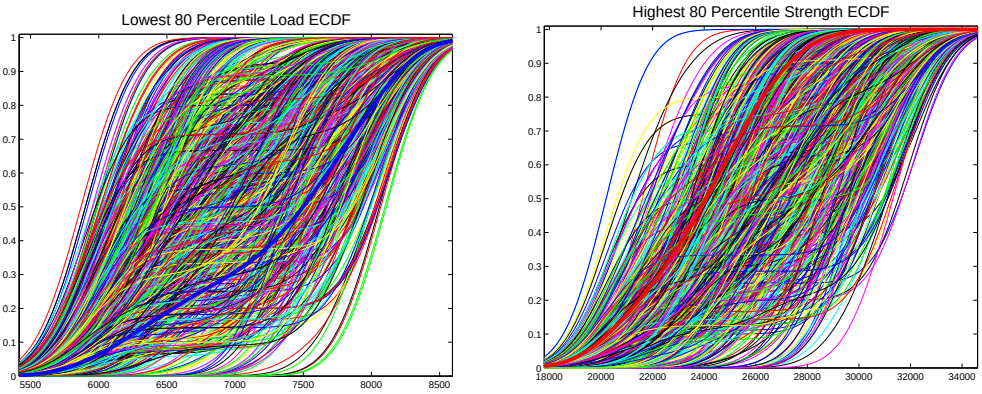

Figure 3.2: KDE estimates for CDFs for load (left) and strength (right) from 1000 resamplings each. The low 20% load and the high 20% strength distributions are shown in thick blue and red lines, respectively.

As before, our analysis used $\alpha = 0.2$ and $M = 13500$ to obtain an 80 *percent* confidence that $P_F\left(X + 13500 > Y\right) \leq 0.11$. This result is very near the confidence level calculated using the discrete representations.

Again, the fact that one can perform estimates of confidence of PEM for two such different distribution forms and achieve such similar results, argues to the robustness of the PEM approach.

About the Bootstrap Method Employed Here

The bootstrap is a method for estimating the sensitivity of a distribution to perturbations on the finite sample set from which that distribution is estimated.

The bootstrap may be used to estimate a $(1-\alpha)\times 100\,percent$ confidence limit on the PEM, ($P_F(M)$ in Equation 2.2). The bootstrap procedure follows:

1. Generate N_B bootstrap samples from the load data, and N_B statistically independent bootstrap samples from the strength data. (N_B is a large number; 1000, for example.)
2. For each bootstrap sample, $b = 1,\ldots,N_B$:
   (a) Fit the bootstrap sample of the load data with a distribution and fit the bootstrap sample of the strength data with a distribution. (We use two distribution types to illustrate in this section: discrete step functions and KDE.)
   (b) Evaluate the PEM, Equation 2.2, and store the result in an $N_B \times 1$ array, $\hat{P}$. The array consists of bootstrap replicates of the PEM statistic.
3. Sort the array $\hat{P}$ in ascending order.
4. Evaluate the quantity in the sorted array that occupies the $(1-\alpha)N_B^{th}$ position, $\hat{P}_{(1-\alpha)N_B^{th}}$.

The quantity evaluated in step 4 is the bootstrap estimated $(1-\alpha)\times 100\,percent$ confidence limit on the PEM. This represents a traditional frequentist confidence limit. If the entire procedure is repeated, $(1-\alpha)\times 100\,percent$ of the estimated PEMs will be less than $\hat{P}_{(1-\alpha)N_B^{th}}$.

A much more extensive discussion of the bootstrap technique is presented in Appendix D.

Chapter 4

Validation

Any model whose use will have important consequences should be validated prior to its exercise in practice. For example, models that will be used to make important decisions regarding operations that may affect human life or safety, or operations that may lead to great expense, should failure occur, ought to be validated. Validation is defined as "the process of determining the degree to which a computer model is an accurate representation of the real world from the perspective of the intended model applications,"[1, 3, 14]. The validation process has been outlined in many papers, for example [5, 4, 16, 18]. Because validation information is generally known statistically, it is appropriate to employ statistically-based validation criteria. (Comments [1] in [19] are particularly cogent.) The PEM framework indeed makes a statistical approach to validation quite natural.

Prior to performance of a validation comparison, the validation must be planned. During the planning phase, the validation team must:

- Specify the model use and purpose
- Specify validation experiments
- Specify the model
- Specify the physical system response measures of interest
- Specify the validation metrics
- Specify the domain of comparison
- Specify the calibration experiments (Calibration is the operation during which model parameters that can be identified only through experiments are estimated.)
- Specify the adequacy criteria (validation requirements)

[1] "Given the crucial importance of model validation in deciding the utility of a simulation for use in operational test, it is surprising that the constituent parts of a comprehensive validation are not provided in the directives concerning verification, validation, and accreditation. A statistical perspective is almost entirely absent in these directives."

An important principle of validation is that experiments that are performed to calibrate the parameters of a model must not be used as the reference against which model predictions are made to validate a model. In other words, validation experiments must be different and should be of a different type than calibration experiments.

After planning a model validation we proceed to complete the steps required to determine the validity of the model:

1. Perform calibration experiments and calibrate model.
2. Perform validation experiments and transmit experimental information to modelers. (In structural dynamics, for example, these are boundary conditions, initial conditions, applied loads, etc.)
3. Generate model-based predictions.
4. Perform validation comparisons and judge validity of model.
5. Take action with respect to intended use of model.

A Motivating Structural Mechanics Example

As specified in the bulleted list at the beginning of this section, in order to validate a structural model, it is necessary to perform experiments on the structure the model is meant to represent and to generate corresponding model predictions. Structural mechanics problems often involve investigating the response of an object to shaking or vibrations. In Figure 1.1 we sketched a structure with linear dampers except for the non-linear spring connecting DOF 5 and DOF 21. In this completely simulated example of a validation, we use two slightly different models. The full model contains a non-linear spring between DOF 5 and DOF 21; this is called the Truth model and is used to simulate the experimental data. The second model approximates the non-linear spring and the damper adjacent to it with a linear spring and a different damper; this is called the linear model. It is used to simulate model predictions. For purposes of validation, we choose to excite the Truth model and its linear approximate model using a classical shock, namely a compensated random haversine (The analysis of both the Truth Model and its linear approximation are provided in Appendix E. Compensation is a modification of the haversine shock that permits its use on a shaker; a compensated shock has first and second integrals that equal zero.) The following analysis seeks to validate the adequacy of the linear model to predict an aspect of the response of the Truth Model.

We are interested in how well this structure survives shocks. In particular, it is required that the absolute peak of acceleration be less than the measured strength of DOF 26. The strength of the component whose critical response measure is peak acceleration of DOF 26 is known only through

experimental measurements. The PDF of strength at DOF 26 is approximated by the KDE of the measured data; the KDE shown in Figure 4.1, and summarizes the true aleatory uncertainty in the strength of DOF 26.

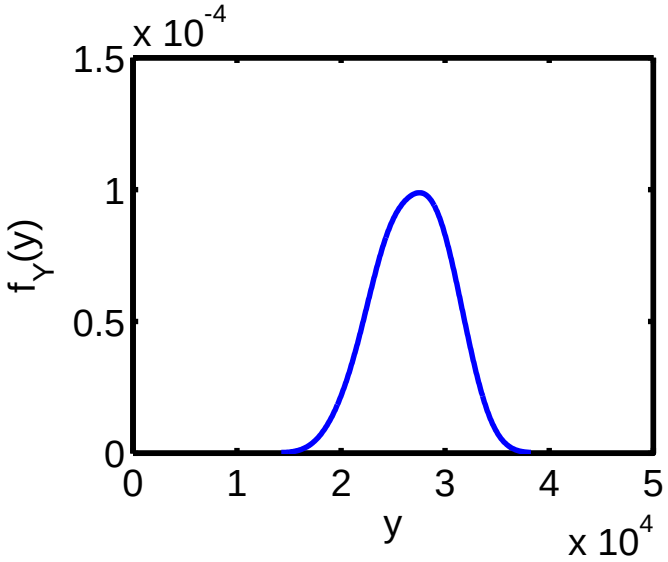

Figure 4.1: KDE of measured strength at DOF 26. The strength is specified in terms of peak accelerations sustainable by the structure at that location.

The haversine shocks that excite the structure come from a source with random amplitude and random duration. The following distributions summarize the characteristics of these shocks. The amplitude is a normally distributed random variable with mean and variance $(3000, 600^2)$; the units of the shock are in/sec^2. The duration of the shocks is a normally distributed random variable, independent of the amplitude, with mean and variance $(0.01, 0.002^2)$; the units of duration are *seconds*. Thirty realizations of the structural excitations used during validation experiments are shown in Figure 4.2. These represent experimental excitations.

A realization of the Truth Model is excited by each realization of the random shock in Figure 4.2. The shock responses of the Truth Model at DOF 26 are shown in Figure 4.3. Units of the responses are in/sec^2.

Generally, we expect to be able to generate more numerical simulations than the number of physical experiments because the latter require hardware, and therefore, involve substantial expense. Here, for purposes of demonstration, our "experimental" data were generated, and consist of the 30 excitation and response accelerations shown in Figures 4.2 and 4.3, respectively. We generate model predictions by choosing randomly among the 30 experimental inputs and using each selected input to excite a realization of a stochastic linear model of the structure. For this demonstration, we choose to generate 100 stochastic linear models and analyze their responses. The acceleration responses of the stochastic, linear structures at DOF 26 are shown in Figure 4.4.

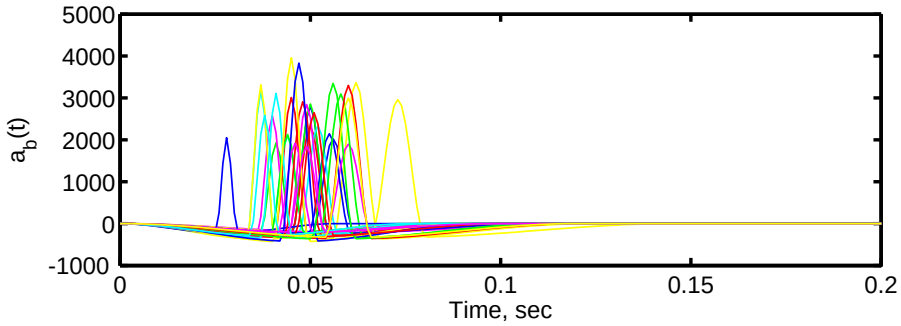

Figure 4.2: Thirty realizations of the compensated, random haversine shock excitation used during validation.

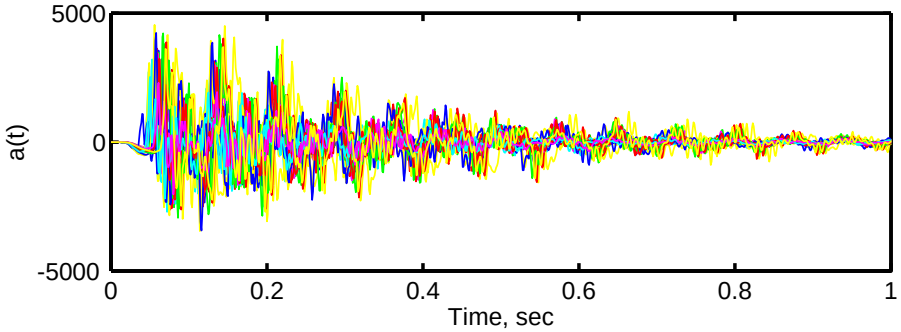

Figure 4.3: Thirty realizations of response of the stochastic Truth Model excited by the thirty realizations of shock excitation in Figure 4.2.

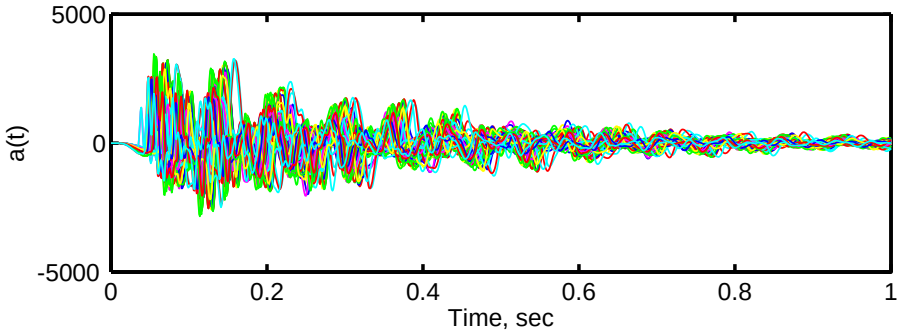

Figure 4.4: One-hundred realizations of response of the stochastic linear structure to randomly chosen excitation realizations from the collection of inputs in Figure 4.2

The data generated here will now be used in a validation. Specifically, peak acceleration responses predicted by the linear model will be compared to peak acceleration responses realized by the Truth Model. Figures 4.5 and 4.6 show the KDEs of the peaks in the absolute values of accelerations at DOF 26 in the Truth model and the linear model, respectively. (Here by "KDEs" we mean the KDE approximations of the PDFs of the relevant random variables.) The probability distribution of the acceleration peaks predicted by the linear model clearly under-predicts slightly the acceleration peaks realized in the Truth Model responses. The current validation seeks to gauge the importance of that under-prediction.

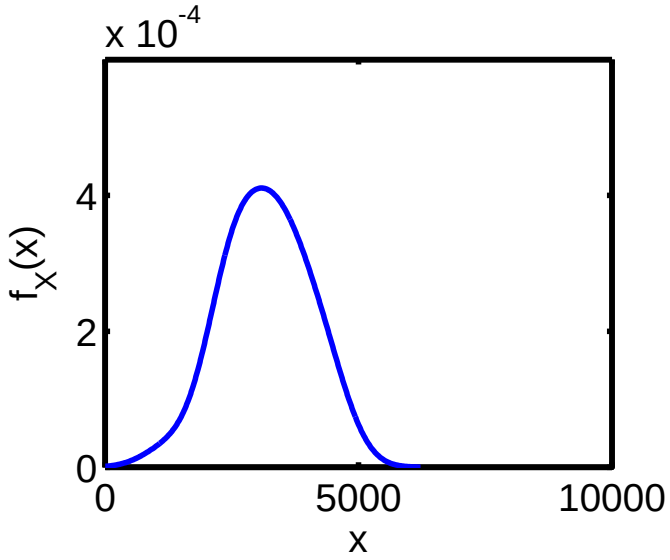

Figure 4.5: KDE of peaks in absolute value of acceleration response at DOF 26 in the Truth Model.

Use of PEM in a Validation Metric

The PEM, defined in Equation 2.2, is devised to involve minimal dependence on the tails of load and strength distributions, and that quality makes it a stable measure of response for use in characterization of experimental and model-predicted responses. In this section, we focus on the PEM, $P_F(M)$, as the system response measure of interest. As before, M is selected to be sufficiently large to assure that calculation of $P_F(M)$ will be reasonably independent of the distribution tails. There are few restrictions on what the system response measure of interest can be. Frequently a direct measure of response such as acceleration, velocity or displacement is chosen. However, when the model will be used to predict structural reliability or probability of failure, use of PEM as the measure of interest is much more appropriate. Our objective is not to show how to plan and perform an entire validation, but rather:

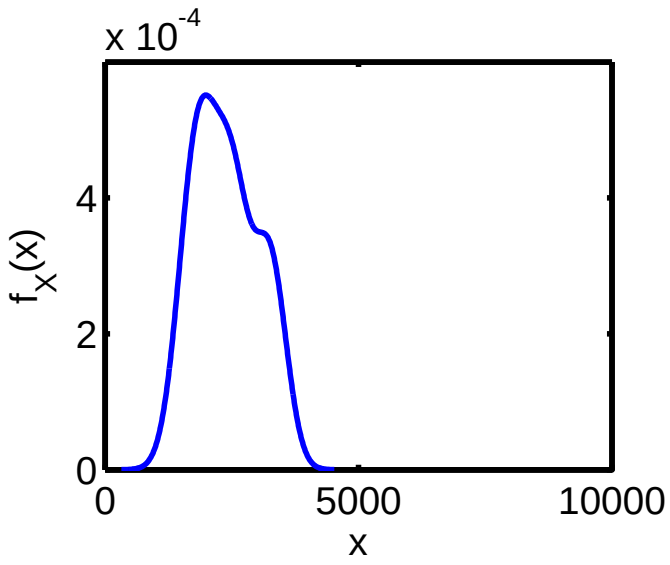

Figure 4.6: KDE of peaks in absolute value of acceleration response at DOF 26 in the linear model.

- To show how PEM can serve as the response measure of interest.
- To illustrate how a validation metric can be formed using the PEM from a physical experiment and the PEM from a model-prediction, and
- To demonstrate how a rational validation requirement can be specified with physically-based and model-based PEMs, and, given that, how model validity might be judged.

The validation metric is a function of the values of $P_F(M)$ computed using "experimental" data from the Truth Model, $P_F^{(\mathrm{Exp})}(M)$, and model-generated data from the linear approximation of the Truth Model, $P_F^{(\mathrm{Mod})}(M)$. In general, when any model of a physical system under-predicts (but not by too great a margin) the chance of safety of a design, then the model is conservative. When the model of the physical system accurately predicts the chance of safety of a design, then the model is accurate. And when the model of the physical system over-predicts the chance of safety of a design, then the model is unconservative (or, not conservative) We judge the limits of acceptability of our estimate of $P_F^{(\mathrm{Mod})}(M)$ with respect to the estimated statistical variability of $P_F^{(\mathrm{Exp})}$ and our appetite for over-conservatism of the model.

Numerous sensible validation metrics are available. We choose to define the validation metric:

$$v_M = \log\left(\overline{P_F^{(\mathrm{Mod})}(M)} \,/\, \overline{P_F^{(\mathrm{Exp})}(M)}\right) \tag{4.1}$$

where $\overline{P_F^{(\mathrm{Mod})}(M)}$ is our best, data-based estimate of PEM predicted by the model, and $\overline{P_F^{(\mathrm{Exp})}(M)}$ is our best, data-based estimate of PEM obtained from experimental data. When the metric is negative, the model under-predicts PEM; this is unconservative because the physical system is less safe than predicted. When the metric becomes too small, this is an unfavorable condition. When the metric is near zero, the model is accurate. When the metric is positive, the model over-predicts PEM; this is conservative because the physical system is safer than predicted. To an extent, this circumstance is favorable, but when the metric becomes too large, this is an unfavorable condition.

The validation requirement, as may be inferred from the discussion, above, is written

$$v_{\min} \leq v_M \leq v_{\max} \tag{4.2}$$

Negative v_M implies model under-conservatism, therefore, the magnitude of $v_{\min}$ should be specified based on the statistical variability of the validation metric, v_M. The statistical variability in v_M can be approximately assessed using bootstrap analysis. The upper limit, $v_{\max}$, implies model conservatism, therefore, it should be specified on the basis of statistical variability of v_M, and the validation team's appetite for over-conservatism of the model.

To perform a validation analysis we use the data of the previous section of this chapter. That section showed that when the Truth Model is excited by a compensated haversine its DOF 26 executes the acceleration responses in Figure 4.3. The peaks of those acceleration responses were gathered and their KDE was computed; it is shown in Figure 4.5. The stochastic linear model was also excited using the compensated haversine, and its DOF 26 acceleration responses were computed; they are shown in Figure 4.4. The acceleration peak responses were gathered and their KDE was computed; it is shown in Figure 4.6.

When the data leading to the KDEs of Figures 4.5 and 4.6 are used to approximate the complementary CDFs (CCDF) of load for the Truth Model and the linear model, and when these CCDFs are used with the KDE approximating the PDF of system strength in Equation 2.2, we obtain the PEMs for the Truth Model and the linear model. They are:

$$\overline{P_F^{(\mathrm{Mod})}(M)} = 0.0357 \qquad \text{and} \qquad \overline{P_F^{(\mathrm{Exp})}(M)} = 0.0584 \tag{4.3}$$

where the margin used in the example is $M = 17,555$

We use these quantities in the formula for the validation metric, Equation 4.1 to obtain:

$$v_M = \log(0.0357/0.0584) = -0.492 \tag{4.4}$$

In order to establish adequacy – perhaps accuracy – of the model predictions, it is necessary to establish the scale of statistical variation of v_M based on experimental data, and judge whether or not the realized validation metric of Equation 4.4 lies within rational limits inferred from experimental variability. To accomplish this task we use the bootstrap. To implement the bootstrap, let $x_i, i = 1,\ldots,30$ denote the peaks in absolute value of the acceleration response at DOF 26

during 30 validation experiments; these are load data, samples from the random variable, X. Let y_j, $j = 1,\ldots,25$ denote the strengths of systems obtained from experiments; these are samples from the random variable Y. The bootstrap procedure is:

1. Collect a bootstrap sample from the load data. (A bootstrap sample is a sample of 30 of the x_i, $i = 1,\ldots,30$, taken with replacement.)

2. Estimate the CCDF of X using the bootstrap sample. This is a bootstrap replicate of the CCDF of X.

3. Collect a bootstrap sample from the strength data.

4. Estimate the PDF of Y using the bootstrap sample. This is a bootstrap replicate of the PDF of Y.

5. Use the bootstrap replicate of the CCDF of X and the bootstrap replicate of the PDF of Y in Equation 2.2 to obtain a bootstrap replicate of the PEM, $\overline{P_F^{(\mathrm{Exp})}(M)}^{(b)}$

6. Use the bootstrap replicate of the PEM from experimental data, $\overline{P_F^{(\mathrm{Exp})}(M)}^{(b)}$, along with the estimate of the PEM from model prediction, $\overline{P_F^{(\mathrm{Mod})}(M)}$, in Equation 4.4 to obtain a bootstrap replicate of the validation metric, $v_M^{(b)} = \log\left(\overline{P_F^{(\mathrm{Mod})}(M)} \,/\, \overline{P_F^{(\mathrm{Exp})}(M)}^{(b)}\right)$.

7. Repeat the process of steps 1 through 6 a large number, B, of times to obtain $v_M^{(b)}$, $b = 1,\ldots,B$.

8. Compute the KDE of the $v_M^{(b)}$, $b = 1,\ldots,B$. This is an approximation of the sampling distribution, $f_{V_M}(u)$, $-\infty < u < \infty$ of the statistic, V_M, the random variable from which the validation metrics defined in Equation 4.4 arise during separate random experiments. (Pairs of percentage points of the PDF of V_M form confidence intervals on the values the realizations v_M might assume.)

9. Compute the $\left[\alpha/2, 1-\alpha/2\right] \times 100\%$ percentage points, $\left[u_{\alpha/2}, u_{1-\alpha/2}\right]$ of the sampling distribution of V_M. These form the basis for defining the limits on the validation requirement.

10. Define the validation limits.

    (a) Assume that in the present case $u_{\alpha/2}$ has a negative value. Then we might define $v_{\min} = u_{\alpha/2}$. Small values of the validation metric imply the potential for an unconservative model, therefore, the only factor that justifies a negative validation metric is random variability in the experiment.

(b) A minimal value for $v_{\max}$ is $u_{1-\alpha/2}$. Because positive values of the validation metric imply a conservative model, validation teams may find a limit higher than $u_{1-\alpha/2}$ to be acceptable. For example, we may set $v_{\max} = \beta u_{1-\alpha/2}$, where $\beta > 1$. The quantity β might reasonably be set at 2, in practical applications.

(c) Set the validation requirement: $[v_{\min}, v_{\max}] = \left[u_{\alpha/2}, \beta u_{1-\alpha/2}\right]$

We performed an example model validation using the Truth Model and linear model simulations described above. The margin was again set to $M = 17{,}555$. The approximation to the sampling distribution of V_M obtained during the course of the analysis is shown in Figure 4.7. It is based on $B = 500$ bootstrap samples. We chose to base the validation requirement on a $[1,99] \times 100\%$ confidence interval on V_M. These limits were computed, and are shown by the red hash marks in Figure 4.7. The red star shows the best estimate of validation metric from Equation 4.4. The percentage points are $[u_1, u_{99}] = [-1.621, 2.300]$. Finally we deemed over-conservatism of the linear model by a factor of 2 to be acceptable. The validation requirement is:

$$[v_{\min}, v_{\max}] = [-1.621, 4.600] \tag{4.5}$$

Based on this criterion, the model is judged valid because $-0.492 \in [-1.621, 4.600]$. In fact, the linear model might be judged accurate based on this criterion.

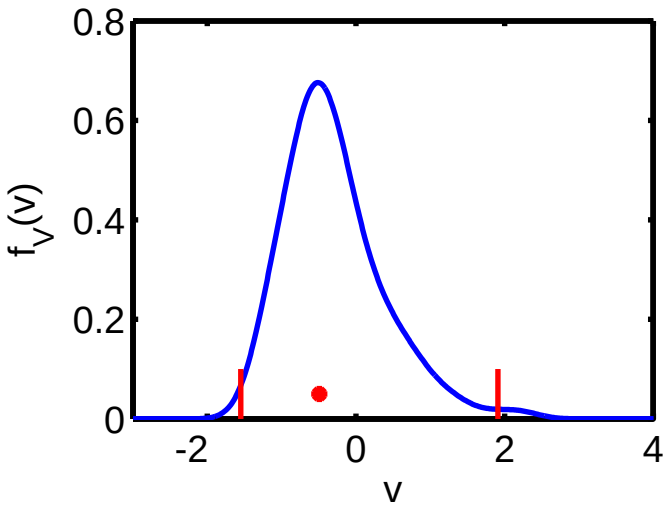

Figure 4.7: KDE of the sampling distribution of the validation metric where the experimental values of load and strength are re-sampled. The red ticks are the one and ninety-nine percent percentage points. The red star denotes the value of the best estimate of the validation metric.

This page intentionally left blank.

Chapter 5

On Making Conservative Predictions

We have presented above a formalism for defining Margin and PEM and confidence in PEM which involves minimal dependence on information in the tails of the distributions. Additionally, we have presented measures for assessing the adequacy of the models, accommodating both aleatoric and epistemic uncertainty.

We are now in a position to use our models, but we would like to be able to use them in a manner that results in *conservative* predictions. Such an approach is developed in the following.

A Triangle Inequality

Say that f_X is an approximation for the load PDF obtained from the experimental realizations $\{x_k\}$, that f_Y is an approximation for the strength PDF obtained from the experimental realizations $\{y_k\}$, and f_Z is an estimate for the load PDF generated by many simulations of our model. These are all shown notionally in Figure 5.1.

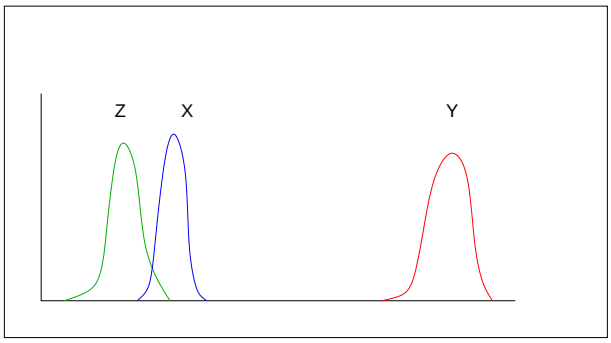

Figure 5.1: *Approximations for the Probability Density Function (PDF) of load, f_X (in blue), the PDF of strength f_Y (in red), and the PDF of model load predictions, f_Z. In this case, the model is distinctly non-conservative.*

In this case, the model is distinctly non-conservative - the predictions of load are generally

lower than the experimental load data. Still, as shown in the previous chapter, the load model could still be considered valid on the basis of the key requirements: it is based on a plausible physics model whose predictions are repeatedly found to be very close to corresponding experimental data.

Whether our model is found to be unconservative, conservative, or accurate, aleatoric uncertainty might easily result in our *predictions* not being conservative. To address that issue, we introduce a quantity M_M so that

$$P(Z + M_M < X) < \beta_M \tag{5.1}$$

where typically $0 < \beta_M \ll 1$.

Quantity M_M is the margin that must be added to the model predictions in order to make the resulting predictions conservative. This is illustrated notionally in Figure 5.2. With margin M_M,

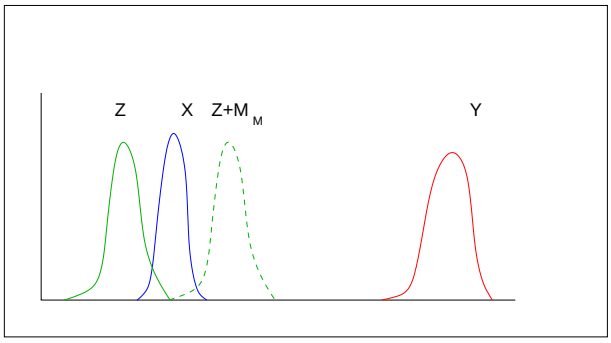

Figure 5.2: *A statistical metric for M_M that assures statistically conservative predictions.*

the model is distinctly conservative in the sense that the probability of random variable $Z + M_M$ being less than the load X (another random variable) is less than β_M. Note that if the model already is *very* conservative, M_M may be a negative number; then the following analysis may be considered unnecessary.

In the sense discussed earlier in this monograph, the model predicts (to within its capabilities) a probability of failure with respect to a margin M_P

$$P(Y < Z + M_P) < \beta_P \tag{5.2}$$

where typically, $0 < \beta_P \ll 1$. All the above probabilities are evaluated as set forth in Equation 2.2.

We shall use inequalities 5.1 and 5.2 to make a statement about the probability of load X exceeding strength Y. Let $\overline{Z} = Z + M_M$ and $\overline{Y} = Y + M_M - M_P$. Equation 5.1 becomes

$$P(\overline{Z} < X) < \beta_M \tag{5.3}$$

and Equation 5.2 becomes

$$P(\overline{Y} < \overline{Z}) < \beta_P \tag{5.4}$$

The theorem proved in Appendix C yields

$$P(\overline{Y} < X) < \beta_M + \beta_P \tag{5.5}$$

which in terms of our original random variables is

$$P(Y < X + M_P - M_M) < \beta_M + \beta_P \tag{5.6}$$

The above sequence shows how the model can be used to predict the probability of failure of our structure subject to the margin associated with the model (M_P) minus the quantity (M_M) added to assure conservatism. The probability of failure is acceptable if $M_P - M_M$ is large enough and $\beta_M + \beta_P$ is small enough, as judged by the persons who must make a decision. Further, most users would wish to assure themselves that the margin, M_M, would hold for model predictions in environments other than those considered, here, and used to define the value, M_M.

The above provides a bound on the reliability of the system in terms of the reliability suggested by our model (expressed in M_P and β_P) and the confidence we place in our model (expressed in M_M and β_M). In terms of the case suggested in Figure 5.1, we have demonstrated a use of a model which is neither accurate nor conservative. Finally, one should observe that the above strategy addresses some of the serious concerns about an absence of statistical or objective meaning in many conventional forms of model validation.

Illustration in our Paradigm Problem

We again examine the model explored in the Validation Chapter of this monograph. The peaks of the absolute value of the acceleration responses at DOF 26 as predicted by our Truth model (30 samples) and by our Linear model (100 samples) were observed, and the KDE approximations to their PDFs were computed. Those distributions were presented in Figures 4.5 and 4.6, respectively and are plotted together in Figure 5.3 for comparison. The square marker identifies the bottom 5% of the linear model and the triangle identifies the top 5% of the truth model.

We see that the model and truth distributions look very similar, especially given the fact that they are both based on limited data, but that is not enough. In the previous chapter we validated the model against "experimental" data. Here we show how model results can be used to make conservative predictions.

For this, we consider the distribution of modified model predictions shown in Figure 5.4. Here we consider the predictions of our model, but with all values increased by a margin $M = 2540$. This margin is that required to align the bottom 5% of the linear model and the top 5% of the truth model.

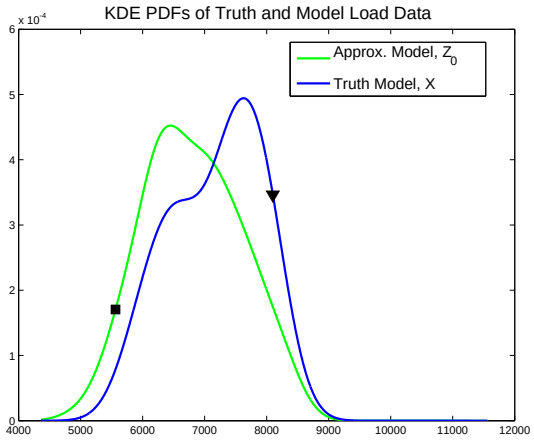

Figure 5.3: Kernel density estimator of the absolute peak of acceleration responses in the nonlinear Truth Model (blue) and the linear model (green) at DOF 26. The square marker identifies the bottom 5% of the linear model and the triangle identifies the top 5% of the truth model.

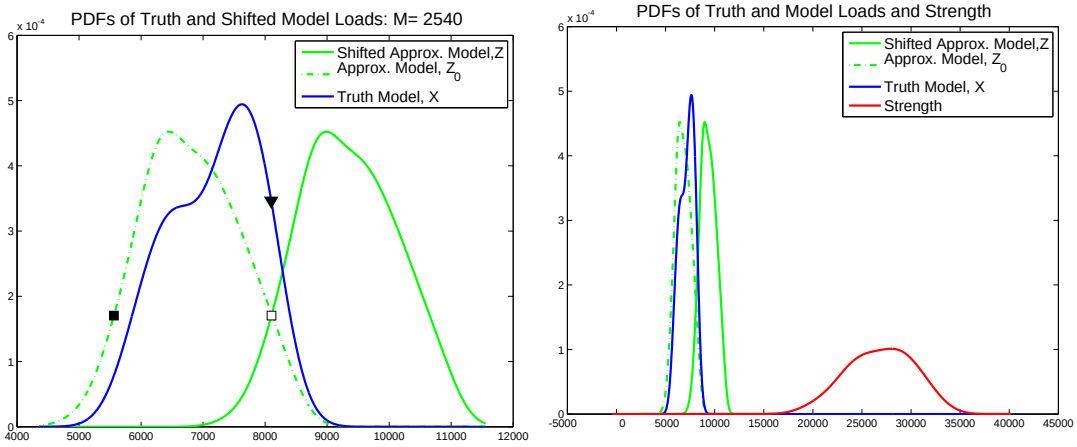

Figure 5.4: Shown on left is the kernel density estimator of the absolute peak of acceleration responses in the nonlinear Truth Model (blue) and the linear model (green) at DOF 26 shifted by a margin $M_M = 2540$. This margin is that required to align the bottom 5% of the linear model and the top 5% of the truth model. The same are shown on the right, along with the KDE estimate for strength.

The probability that the shifted model is conservative is

$$P(Z+M_M > X) = \iint\limits_{z+M_M>x} f_Z(z) f_X(x) dx dz = \int_{-\infty}^{\infty} f_Z(z) \int_{-\infty}^{z+M_M} f_X(x)\, dx\, dz$$

$$= \int_{-\infty}^{\infty} f_Z(z) F_X(z+M_M)\, dz \tag{5.7}$$

Both terms in the integrand of Equation 5.7 are shown in Figure 5.5, where the KDE approximation for f_Z is scaled to make it visible.

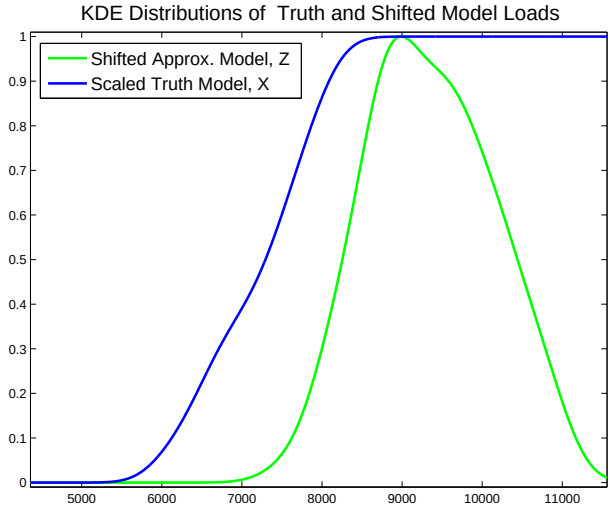

Figure 5.5: The factors $F_X(z+M_M)$ (blue) and $f_Z(z)$ (green) in the integrand of Equation 5.7. Both distributions are estimated using KDE. To put both plots on the same figure, the PDF of Z is normalized by its peak value.

The integral indicated in Equation 5.7 is evaluated numerically: $P(Z+M_M > X) \approx 98.2\%$. That is, the probability of being non-conservative is $\beta_M = 1 - P(Z+M_M > X) \approx 1.8\%$. (The corresponding probabilities when the step functions are used for the CDF and delta functions for the PDF are 99.2% and $\beta_M \approx 0.77\%$, respectively.) Of course, the above quadrature depends tremendously on which sample points were selected. This can be addressed through an analysis of sampling distribution. Resampling employing 1000 samples each, bootstrap sampling was performed on both Truth and Model data sets. The relevant KDE approximations for those distributions were constructed in the manner described earlier (Figure 5.6).

An algorithm similar to that employed earlier is applied to this problem:

1. The integral indicated in Equation 5.7 for $P(Z+M_M > X)$ is evaluated numerically for ordered pairs of Truth CDFs and Model PDF.

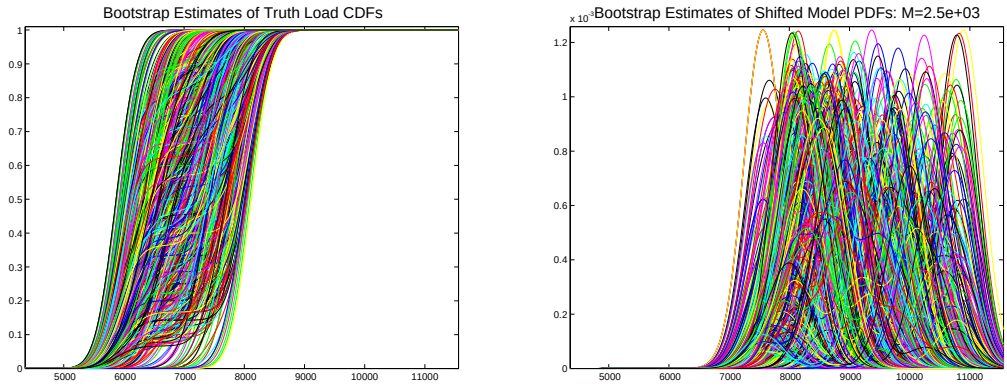

Figure 5.6: KDE estimators for the 1000 bootstraps for CDF of the truth data and for the 1000 bootstraps for PDF of the model data.

2. Those calculated values for $P(Z+M_M > X)$ are stored in an array.

3. The array is sorted in ascending order.

4. For a confidence of β we select the k^{th} element of the sorted array where $k \approx (1-\beta) * N_B$ and N_B is again the number of bootstrap samplings.

For the problem at hand, we desire an 80% confidence in our probability prediction, so we use the 20 percentile term in our array of quadratures. This is illustrated in Figure 5.7. Numerically, we find with 80% confidence that $P(Z+M_M > X) \approx 91.4\%$. The probability of being non-conservative at the same level of confidence is $\beta_M = P(Z+M_M < X) \approx 8.6\%$. The corresponding values when the discrete functions are used for the distributions are 94% and $\beta_M \approx 6\%$, respectively.

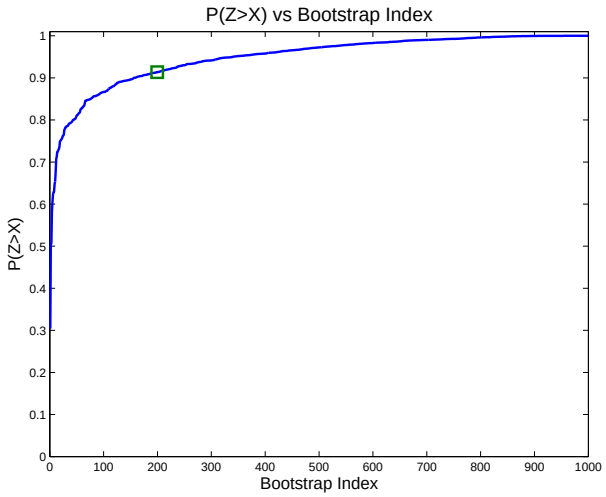

Figure 5.7: The quadratures of Equation 5.7 for the 1000 bootstrap pairs. The 80% confidence is achieved by employing the 20 percentile term.

Reliability Calculations with Approximate Model

Now that we have a metric on the approximate model, we can use it to make calculations relevant to reliability. Analogous to what was done in Section 2, we identify a margin that when added to the load predictions of the linear model permits us to calculate a PEM that is reasonably independent of the forms used to approximate both the load and strength distributions. Again we achieve this by specifying a margin such that the upper 5% of the resulting loads aligns with the bottom 5% of the strengths. The resulting PDFs of loads and strengths, represented by KDE estimators, are shown in Figure 5.8.

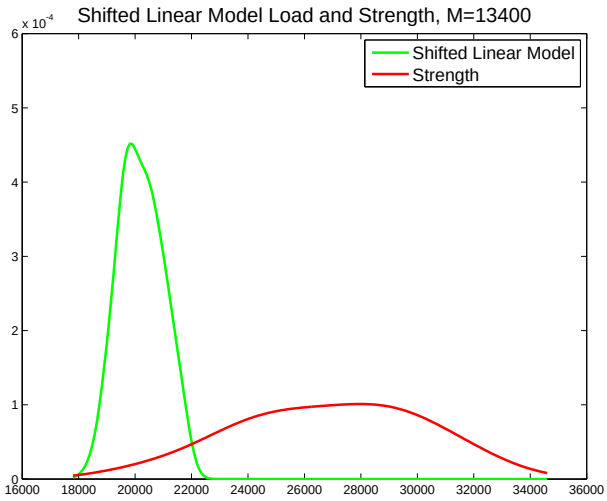

Figure 5.8: The linear model shifted by margin 13400 so that the upper 5% of the resulting load aligns with the bottom 5% of the strengths. Both PDFs are represented by KDE expansions.

Numerical evaluation of Equation 2.2 for this margin and for KDE expansions for load and strength distributions yields a probability of model predictions plus margin ($M_P = 13400$) of $\beta_P = 3.3\%$. When the relevant distributions are represented by step functions and delta functions, the integral evaluates to $\beta_P = 2.3\%$.

Again, we really need a Probability of Exceeding Margin that is accompanied by some confidence estimate. Again, this is achieved by performing bootstrap resamplings of loads and strengths. For our example problem, when we employ 1000 bootstrap resamplings and KDE expansions for the distributions, we obtain an 80% confidence that the PEM is less than $\beta_P = 6.9\%$. When discrete expressions for the distributions are employed, our estimate is that we have a 80% confidence that the PEM is less than $\beta_P = 4.2\%$.

Employing the triangle inequality of earlier in this chapter and the quadratures where we used KDE expansions for the distributions and recalling that $M_M = 2540$, we may make the following

assertion with 80% confidence

$$P(X + 13400 - 2540 > Y) < 6.9\% + 8.6\%$$

$$P(X + 10860 > Y) < 16\% \tag{5.8}$$

The corresponding statement where we use discrete expressions is

$$P(X + 13400 - 2540 > Y) < 4.2\% + 6\%$$

$$P(X + 10860 > Y) < 10\% \tag{5.9}$$

again, with 80% confidence.

We may make two observations here:

1. These two statements for probability of exceeding margin are very close to each other, despite the very different forms assumed for the distributions. This is a feature of the theme of this monograph.

2. These statements, though far from the statements of traditional reliability theory which may involve probabilities of failure on the order of 10^{-6}, may be as much as one can actually say with confidence on the basis of sparse data.

This page intentionally left blank.

Chapter 6

Margin, Margin, and Margin

We have spoken about the distinction between design margin (a target) and achieved margin. Further, uncertainty causes us to refer to the sampling distribution of achieved margin. When we account for sampling or aleatoric uncertainty, we then talk about yet another margin that is associated with a confidence value.

There is yet one more perspective on margin: the engineering view. Of the above margins, the first is aspirational and the rest are based on statistics. There are questions that can be addressed only with an understanding of the relevant physics:

1. Are the statistically supported margins (even the ones with confidence values) actually reliable from an engineering standpoint? Even when all statistical experience and all known aleatoric uncertainty filtered through postulated model forms assure a large margin, understanding of the physics is necessary to know that that margin is sustainable. This notion is illustrated in Figure 6.1.

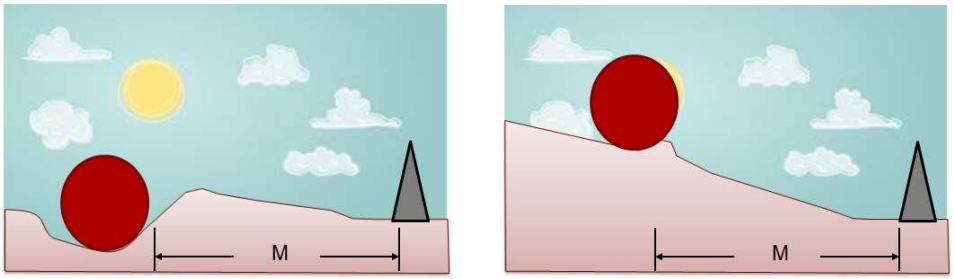

Figure 6.1: Two different circumstances that may have the same statistically assured margins. Consideration of the underlying physics shows them to be associated with entirely different assessments of jeopardy.

2. Whether a statistically supported margin is sufficient to meet the goals of an engineering design is an engineering question. It must be addressed through both programmatic and physical considerations.

This page intentionally left blank.

Chapter 7

Conclusion

We have introduced here an integrated treatment of margin, probability, and confidence. This approach is intuitive both in concept and implementation. As part of this development, we introduced a statistically meaningful notion of validation. This definition provides a methodology for justifying the use of models as engineers and designers are inclined to use them, provided that their predictions maintain a systematic relation with reality.

One very strong feature of this approach is that it obviates the need to postulate the forms of the relevant distributions. In particular, the hazard of extrapolating beyond the known data points into the tails of the distribution is largely removed. The resulting probabilistic statements do not have the reassuring sound sometimes resulting from traditional reliability calculations such as "The probability of failure is less than one in a million". Indeed the analysis presented here argues that such statements cannot be meaningful. This is consistent with a famous statement of Richard P. Feynman[1] [12].

We developed, using the same general approach, a metric for assessing model validity and a strategy to assuring conservative predictions from that model. Both of these approaches benefit from having minimal dependence on the tails of the relevant distributions.

There is much left to be done, including extension of this approach to multidimensional analysis and testing of these techniques on real problems.

Finally, we note that no matter how the statistics of models and experiments is handled, there remains the irreducible issue of extrapolation of testable results into domains where testing is not possible. Confidence in such extrapolations can come only through both thorough investigation of the relevant physics and very careful treatment of all data.

[1] "If a guy tells me that the probability of failure is 1 in 10^5, I know he's full of crap"

This page intentionally left blank.

References

[1] American Institute of Aeronautics and Astronautics Staff. AIAA guide for the verification and validation of computational fluid dynamics simulations. Technical Report AIAA G-077-1998, American Institute of Aeronautics and Astronautics, 1998. ISBN: 1563472856.

[2] Alfredo Hua-Sing Ang and Wilson H. Tang. *Probability Concepts in Engineering Planning and Design: Volume I - Basic Principles*. John Wiley & Sons, 1975.

[3] ASME. Guide for verification and validation in computational solid mechanics, an American national standard. Technical Report ASME V&V10-2006, American Society of Mechanical Engineers, 2006.

[4] Ivo Babuška and J. Tinsley Oden. V&V in computational engineering and science. Part 1: Basic concepts. Technical Report ICES Report 03-52, DTIC Document, Institute for Computational Engineering and Sciences (ICES) The University of Texas at Austin, 2003.

[5] Ivo Babuška and J. Tinsley Oden. The reliability of computer predictions: Can they be trusted? *Int. J. Numer. Anal. Model*, 3:255–273, 2006.

[6] Jack R. Benjamin and C. Allin Cornell. *Probability Statistics and Decision For Civil Engineers*. McGraw Hill Book Co., 1970.

[7] Duane C Boes, F.A. Graybill, and A.M. Mood. *Introduction to the Theory of Statistics*. Series in Probability. McGraw-Hill, New York, 3 edition, 1974.

[8] B. Efron and R. Tibshirani. *An Introduction to the Bootstrap*. Monographs on Statistics and Applied Probability. Chapman & Hall, 1993.

[9] Bradley Efron. Bootstrap methods: another look at the jackknife. *The Annals of Statistics*, 7(1):1–26, 1979.

[10] Bradley Efron. Computer and the theory of statistics: thinking the unthinkable. *SIAM Review*, 21(4):460–480, 1979.

[11] William Feller. *An Introduction to Probability Theory and Its Applications*, volume 1. John Wiley & Sons, Inc., 3 edition, 1968.

[12] Richard Phillips Feynman. *What Do You Care What Other People Think?: further adventures of a curious character*. W. W. Norton & Company, 1988. ISBN 0-393-02659-0.

[13] R. A. Fisher and L. H. C. Tippett. Limiting forms of the frequency distribution of the largest or smallest member of a sample. *Mathematical Proceedings of the Cambridge Philosophical Society*, 24:180–190, 1928.

[14] Raymond Jeanloz. Science-based stockpile stewardship. *Physics Today*, 53(12):44–49, 2000.

[15] I. Miller and J.E. Freund. *Probability and Statistics for Engineers*. Prentice-Hall, Englewood Cliffs, NJ, USA, 2nd edition, 1977.

[16] J. Tinsley Oden, Robert Moser, and Omar Ghattas. Computer predictions with quantified uncertainty, Part 2. *SIAM News*, 43(10):1–4, Dec. 2010.

[17] Committee on the Evaluation of Quantification of Margins, Uncertainties Methodology for Assessing, and National Research Council Certifying the Reliability of the Nuclear Stockpile. *Evaluation of Quantification of Margins and Uncertainties Methodology for Assessing and Certifying the Reliability of the Nuclear Stockpile*. The National Academies Press, 2008.

[18] Thomas L. Paez. Introduction to model validation. In *Proceedings of the IMAC-XXVII, Held February 9-12, 2009 Orlando, Florida USA*. Society for Experimental Mechanics, 2009.

[19] Panel on Statistical Methods for Testing and Evaluating Defense Systems, Committee on National Statistics, National Research Council. *Statistics, Testing, and Defense Acquisition: New Approaches and Methodological Improvements*. The National Academies Press, 1998.

[20] Emanuel Parzen. On estimation of a probability density function and mode. *Ann. Math. Statist.*, 33(3):1065–1076, 1962.

[21] Murray Rosenblatt. Remarks on some nonparametric estimates of a density function. *Ann. Math. Statist.*, 27(3):832–837, 1956.

[22] Bernard W Silverman. *Density estimation for statistics and data analysis*, volume 26. Chapman & Hall/CRC, 1986.

[23] Waloddi Weibull. A statistical distribution function of wide applicability. *ASME Journal of Applied Mechanics*, 18(3):293–297, September 1951.

Appendix A

The Distributions Employed in Chapter 1

The distributions used in the explorations of Chapter 1 are all discussed in depth in [6], but their mathematical definitions are summarized here.

1. The normal distribution, also called the Gaussian distribution, is defined by

$$f_X(x) = \frac{1}{\sigma\sqrt{2\pi}} e^{-(x-\mu)^2/2\sigma^2} \tag{A.1}$$

   where μ and σ are the mean and standard deviation of the distribution.

   The corresponding cumulative distribution is:

$$F_X(x) = \frac{1}{2}\left[1 + \text{erf}\left(\frac{x-\mu}{\sigma\sqrt{2}}\right)\right] \tag{A.2}$$

   where erf is the error function: $\text{erf}(x) = (2/\sqrt{\pi})\int_0^x \exp(-t^2)dt$.

2. The log-normal distribution is defined by

$$f_X(x) = \frac{1}{x\beta\sqrt{2\pi}} \exp\left(\frac{(\ln(x)-\alpha)^2}{2\beta^2}\right) \tag{A.3}$$

   where α and β are parameters of the distribution. The mean and standard deviation are: $\mu = \exp(\alpha+\beta^2/2)$ and $\sigma = \left(\exp(\sigma^2)-1\right)\exp\left(\alpha+\beta^2/2\right)$.

   The corresponding cumulative distribution function is

$$F_X(x) = \frac{1}{2}\text{erfc}\left[-\frac{\ln(x)-\alpha}{\beta\sqrt{2}}\right] \tag{A.4}$$

   where erfc is the complementary error function: $\text{erfc}(x) = 1 - \text{erf}(x)$

3. The extreme value distribution - actually the Type I extreme value distribution - is defined by

$$f_X(x) = \frac{1}{\beta}\exp\left[\frac{x-\alpha}{\beta} - \exp\left(\frac{x-\alpha}{\beta}\right)\right] \tag{A.5}$$

where α and β are parameters of the distribution. This is also sometimes called the Gumbel distribution. The mean and standard deviation of this distribution are: $\mu = \alpha - \gamma\beta$ and $\sigma^2 = (1/6)\pi^2\beta^2$ where γ is the Euler constant.

The corresponding cumulative distribution is:

$$F_X(x) = \exp(-\exp(-(x-\alpha)/\beta)) \tag{A.6}$$

Appendix B

Proof with respect to Tails in *PEM*

A major strength of the approach presented here for defining margin and probability of exceeding margin as spelled out in Equation 2.2, is that the calculation has minimal dependence on information in the tails of the distributions. This is the case because the tails contribute very little to the integral. This notion is made rigorous as follows.

B.1 Equations at Hand

For coherence, we re-derive 2.2 here. We define

$$\begin{aligned} P_F(M) &= P[X+M>Y] \\ &= \int_{x+M>y} f_X(x) f_Y(y)\, dx\, dy = \int_{-\infty}^{\infty} f_Y(y) \left(\int_{y-M}^{\infty} f_X(x)\, dx \right) dy \\ &= \int_{-\infty}^{\infty} f_Y(y) \big(1 - F_X(y-M)\big)\, dy \end{aligned} \tag{B.1}$$

Here f_Y is the PDF of RV Y and F_X is the CDF of RV X. The corresponding PDF for X is f_X and the corresponding CDF of Y is F_Y. We presume there that M is chosen so that there is sufficient overlap of f_X and f_Y so that $P_F(M) \gg 0$.

B.2 Defining the Tails

Choose a small ε and define x^- such that

$$F_X(x^-) = \varepsilon \tag{B.2}$$

and define x^+ such that

$$1 - F_X(x^+) = \varepsilon \tag{B.3}$$

Similarly, define y^- and y^+ by

$$F_Y(y^-) = \varepsilon \tag{B.4}$$

and

$$1 - F_Y(y^+) = \varepsilon \tag{B.5}$$

B.3 Surrogate Distributions

Let's define surrogate distributions

$$\tilde{f}_X(x) = \big(H(x-x^-) - H(x-x^+)\big)\, f_X(x) \tag{B.6}$$

and

$$\tilde{f}_Y(y) = \big(H(y-y^-) - H(y-y^+)\big)\, f_Y(y) \tag{B.7}$$

where H is the Heaviside step function. The above functions are the original distributions with the tails lopped off. They are themselves not strictly PDFs because they do not integrate to 1.0.

Let's also define

$$\tilde{F}_X(x) = \int_{-\infty}^{x} \tilde{f}_X(x)\, dx \tag{B.8}$$

Note that

$$F_X(x) - \tilde{F}_X(x) \begin{cases} \leq \varepsilon & \text{for} \quad x < x^- \\ = \varepsilon & \text{for} \quad x^- < x < x^+ \\ \leq 2\varepsilon & \text{for} \quad x^+ < x \end{cases} \tag{B.9}$$

B.4 Bounding the Dependence

Our approach is as follows:

1. Consider arbitrary PDFs f_X and f_Y.
2. Demonstrate that when the tails are deleted, the change in $P_F(M)$ in Equation B.1 is $O(\varepsilon)$ (of order ε).
3. Observe that since this change is of the same order regardless of the content in the tails, the integral as a whole is independent of those tails, modulo a term of $O(\varepsilon)$.

Let's begin.

$$P_F(M) = \int_{-\infty}^{\infty} f_Y(y)\big(1 - F_X(y-M)\big)\, dy$$

$$= \int_{y^-}^{y^+} f_Y(y)\,(1 - F_X(y-M))\,dy + O(\varepsilon) \tag{B.10}$$

because $1 - F_X(x) < 1$ for all x.

$$= \int_{y^-}^{y^+} f_Y(y)\,\left(1 - \tilde{F}_X(y-M)\right)\,dy + O(\varepsilon) \tag{B.11}$$

because $\int f_Y(y)(F_X(y-M) - \tilde{F}_X(y-M))dy \leq \int f_Y(y)\,2\,\varepsilon\,dy = O(\varepsilon)$.

$$P_F(M) = \int_{-\infty}^{\infty} \tilde{f}_Y(y)\,\left(1 - \tilde{F}_X(y-M)\right) + O(\varepsilon) \tag{B.12}$$

We have established that we can ignore the tails at the cost of introducing an error $O(\varepsilon)$ in $P_F(M)$.

This page intentionally left blank.

Appendix C

Transitivity Inequality Proof

Let

$$P(Z < X) < \beta_1 \tag{C.1}$$

and

$$P(Y < Z) < \beta_2 \tag{C.2}$$

It is shown below that

$$P(Y < X) < \beta_2 + \beta_1 \tag{C.3}$$

where X, Y,Z are all independent random variables.

Define some transformations.

$$R = Z - X \qquad S = Y - Z \qquad U = Y - X \tag{C.4}$$

Then the initial specifications translate to

$$P(R < 0) < \beta_1 \tag{C.5}$$

and

$$P(S < 0) < \beta_2 \tag{C.6}$$

The random variable

$$U = R + S \tag{C.7}$$

Therefore, we seek to show, in Eq. (C.3)

$$P(U < 0) = P(R + S < 0) < \beta_1 + \beta_2 \tag{C.8}$$

An event that contains $R + S < 0$ is the event $(R < 0) \cup (S < 0)$. The reason is that when $R + S < 0$, either $(R < 0)$ or $(S < 0)$ or both $(R < 0)$ and $(S < 0)$. But, in addition, the event $(R < 0) \cup (S < 0)$ contains outcomes in which $R + S \geq 0$. In view of this, we can write

$$P(R + S < 0) < P((R < 0) \cup (S < 0)) \tag{C.9}$$

The law of the total event states that the right hand side can be expanded to

$$P(R+S<0) < P((R<0)) + P((S<0)) - P((R<0) \cap (S<0)) \tag{C.10}$$

If we add the final term on the right to the right hand side, only, we make the right hand side larger than it already is, to obtain

$$P(R+S<0) < P((R<0)) + P((S<0)) = \beta_1 + \beta_2 \tag{C.11}$$

Q.E.D.

Appendix D

Bootstrap Resampling

One of the objectives of statistical analysis is the assessment of variability of estimates of the parameters of probability distributions of random variables and random processes [7]. In the "Real-World" framework for variability analysis a sequence of statistically independent, identically distributed random variables $(X_1, \ldots, X_n) = X_j,\ j = 1, \ldots, n$ is sampled once to obtain realizations $(x_1, \ldots, x_n) = x_j,\ j = 1, \ldots, n$. A statistic of the random variables is expressed $g(X_1, \ldots, X_n)$ where $g(\bullet)$ is a deterministic function, i.e., the function has fixed form. The form of the function, $g(\bullet)$, is obtained through a specific analysis, e.g., maximum likelihood analysis, to form an estimator of a particular parameter of a probability distribution. For example, in the case of the mean, $g(X_1, \ldots, X_n) = \bar{X} = \left(1/n\right) \sum_{j=1}^{n} X_j$; the quantity expressed here is the sample mean, and it is a random variable because it is a function of the random variables, $X_j,\ j = 1, \ldots, n$. When we use the formula on the realizations, $g(x_1, \ldots, x_n) = \bar{x} = \left(1/n\right) \sum_{j=1}^{n} x_j$, we obtain a realization of the random variable $\bar{X}$.

In the Real-World we can, in principle, repeat the experiment where a set of realizations, $x_j,\ j = 1, \ldots, n$ is drawn from the source $X_j,\ j = 1, \ldots, n$. Usually, the realizations drawn from the random source on the second trial differ from the realizations drawn on the first (or any other) trial. The sample mean, $\bar{x}$, computed from the second set of realizations differs from the first realization of $\bar{x}$, etc. If a collection of sample mean realizations, $\bar{x}_k, k = 1, \ldots, N$, is generated, that collection will represent the distribution of the random variable $\bar{X}$ and the distribution of $\bar{X}$ might be inferred from the data. At least, the Karhunen-Loeve expansion (KLE) can be written as an estimate to the PDF of $\bar{X}$ and that is an approximate characterization of the distribution of $\bar{X}$

When the random source, $X_j,\ j = 1, \ldots, n$, is normally distributed with mean and variance $\left(\mu_X, \sigma_X^2\right)$, then the sample mean, $\bar{X}$, is also normally distributed with mean and variance $\left(\mu_X, \sigma_X^2/n\right)$. Further, the distribution of the random variable, $t_{n-1} = \left(\bar{X} - \mu_X\right) / \left(S_X/\sqrt{n}\right)$ is Student's t with $(n-1)$ degrees of freedom. The random variable,S_X, is the square root of
$S_X^2 = \left(1/(n-1)\right) \sum_{j=1}^{n} (X_j - \overline{X})^2$; the latter is the unbiased estimator formula for the variance. The distributions specified here could all be easily confirmed if multiple realization sets, $x_j,\ j = 1, \ldots, n$, were collected and analyzed. The sampling distribution (i.e., the probability distribution that samples follow) for the random variable $\left(\bar{X} - \mu_X\right) / \left(S_X/\sqrt{n}\right)$ can be used to establish the standard

error for the mean and confidence intervals for the mean.

Figure D.1 shows the steps to be taken, in the Real World framework, to estimate the sampling distribution of a statistic that estimates an arbitrary parameter, $G = g(X_1, \ldots, X_n)$, of the probability distribution of a random variable when multiple realization sets can be collected.

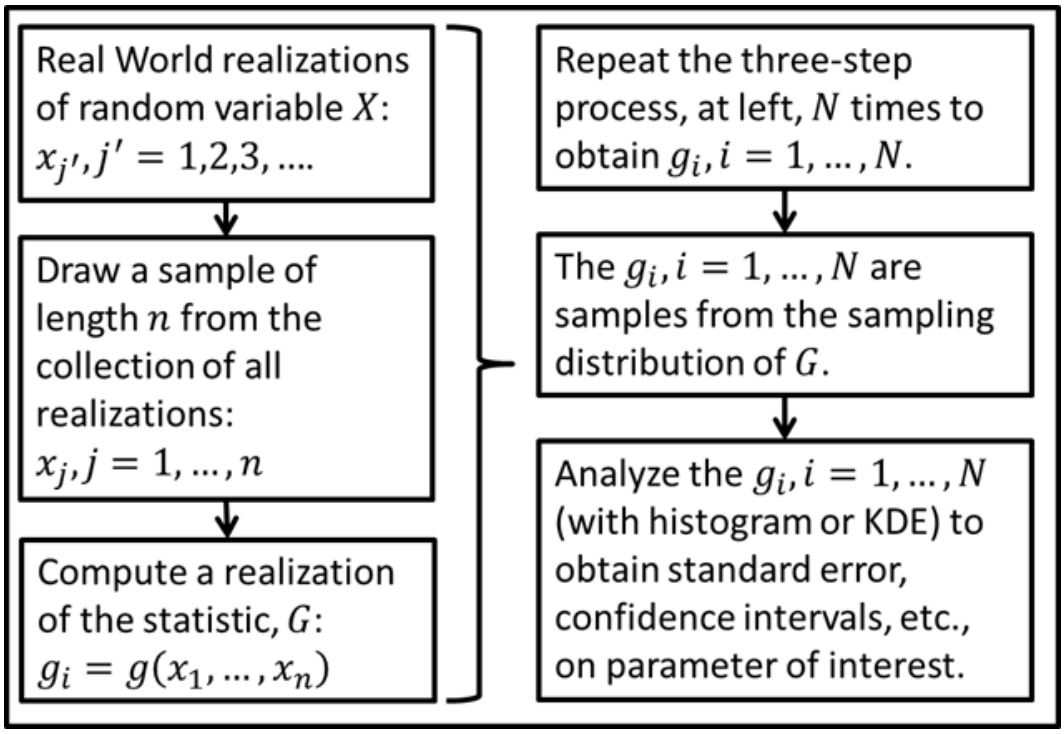

Figure D.1: Procedure for obtaining sampling distribution of an estimator, G.

In spite of all that has been said here, reality dictates that collection of samples costs money, and one sample, only, is typically available. That is why the normal assumption is useful – when it applies accurately. In the case of mean estimation, we are fortunate in the sense that The Central Limit Theorem causes the mean estimator, $\bar{X}$, to have a distribution that converges rapidly to the normal distribution as the number of data, n, increases. That is not always the case for estimators of other parameters. In those cases, other techniques are required to estimate standard errors and confidence intervals for parameters. The bootstrap provides an alternate to classical techniques.

The bootstrap is a numerically intensive technique for the assessment of variability of estimates of the parameters of probability distributions of random variables and random processes [8]. Whereas, in principle, the Real World provides the opportunity to gather multiple sets of samples x_j, $j = 1, \ldots, n$ from a random source X_j, $j = 1, \ldots, n$, the Bootstrap World works with the single set of data x_j, $j = 1, \ldots, n$. The bootstrap framework holds that if we sample x_j, $j = 1, \ldots, n$ multiple times we can explore the variability of estimators. How do we obtain multiple samples from the single sample x_j, $j = 1, \ldots, n$?

We define a bootstrap sample from the data $x_j,\ j=1,\ldots,n$ as a collection $x_i^{(b)},\ i=1,\ldots,n$. The quantity $x_i^{(b)}=x_{j'}$ is a number taken from $x_j,\ j=1,\ldots,n$ such that the subscript j' is a realization of a discrete random variable with equal probabilities on $[1,\ldots,n]$. The sampling is performed "with replacement;" therefore, the sequence $x_i^{(b)},\ i=1,\ldots,n$ may contain repeated values from $x_j,\ j=1,\ldots,n$ and $x_i^{(b)},\ i=1,\ldots,n$ may be missing some values from $x_j,\ j=1,\ldots,n$. It is possible to generate as many bootstrap samples from a collection of data as desired. Because the number of combinations of data in a bootstrap sample is proportional to $n!$ (n factorial) it is unlikely that bootstrap samples will be duplicated, in a practical analysis, once n surpasses 8, or so Next, we define a bootstrap replicate of a statistic as $g_b=g\left(x_1^{(b)},\ldots,x_n^{(b)}\right)$. In the case of the mean estimator this would be $\bar{x}^{(b)}=\left(1/n\right)\sum_{j=1}^{n}x_j^{(b)}$

Bootstrap analysis requires that for a large number, B, we generate B bootstrap samples of the data, $x_i^{(b)},\ i=1,\ldots,n,\ b=1,\ldots,B$, and then compute for each sample the bootstrap replicate of the statistic, $g_b=g\left(x_1^{(b)},\ldots,x_n^{(b)}\right),\ b=1,\ldots,B$. The bootstrap analyzes the computed bootstrap replicates $g_b,\ b=1,\ldots,B$, to establish features of the sampling distribution of the estimator G. For example, the standard error of the estimator may be estimated as the sample standard deviation of the $g_b,\ b=1,\ldots,B$. Confidence intervals may also be estimated.

The procedure for estimation of bootstrap confidence intervals is direct. Denote the CDF estimator formed from the replicates $g_b,\ b=1,\ldots,B$, with $\hat{F}_G(\beta),\ -\infty<\beta<\infty$. This might be, for example, the empirical CDF [11, 15] of the $g_b,\ b=1,\ldots,B$ or it might be the integral of the kernel density estimator [21, 22] However the CDF is estimated, we form the symmetric, two-sided, $(1-\alpha)\times 100\%$ confidence interval estimates by solving for $[L,U]$ in

$$\hat{F}_G(L)=\alpha/2\quad \hat{F}_G(U)=1-\alpha/2 \tag{D.1}$$

This requires inversion of $\hat{F}_G(\beta)$, and that can be accomplished with a search when the CDF is approximated with the empirical CDF, or interpolation when the CDF is estimated based on the KDE. Figure D.2 shows the steps to be taken, in the bootstrap framework, to estimate the sampling distribution of a statistic that estimates an arbitrary parameter, $G=g(X_1,\ldots,X_n)$, of the probability distribution of a random variable when one realization, only, can be collected.

Example 1. Collect $n=10$ data from a random source known to be non-Gaussian. The data are listed here:

-0.951	0.563
-0.721	-0.129
-0.286	-1.083
0.057	0.959
-1.202	-0.951

A histogram of the data is shown in Figure D.3, and the empirical CDF of the data is shown in Figure D.4

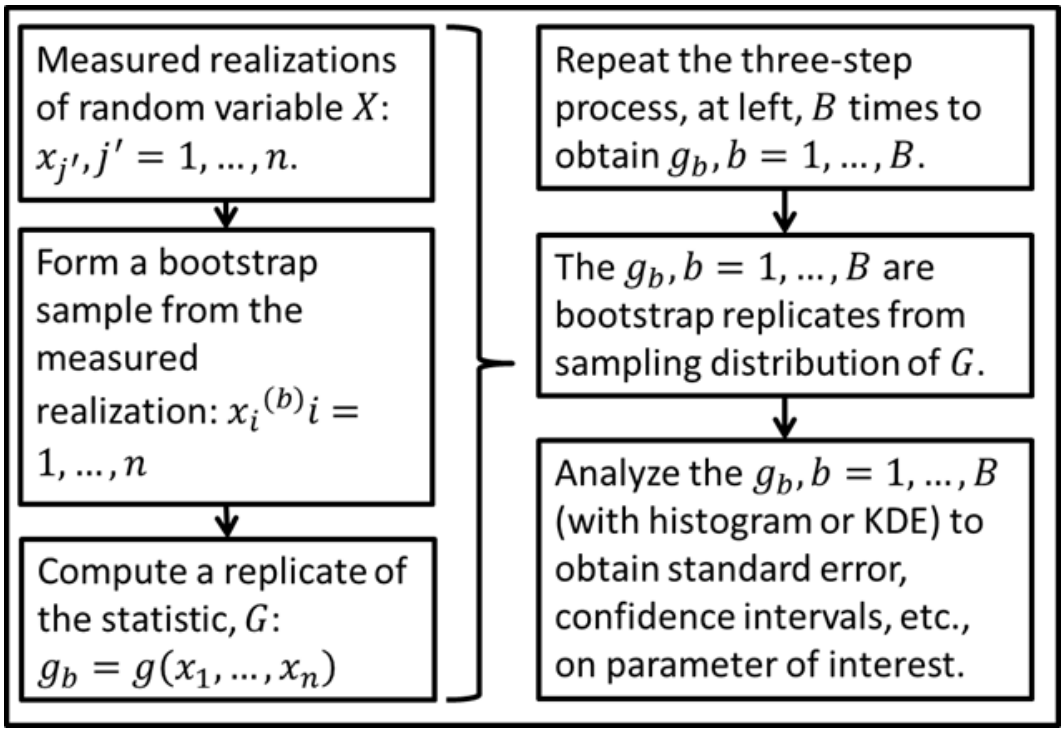

Figure D.2: Procedure for obtaining sampling distribution of an estimator, G., in the bootstrap framework.

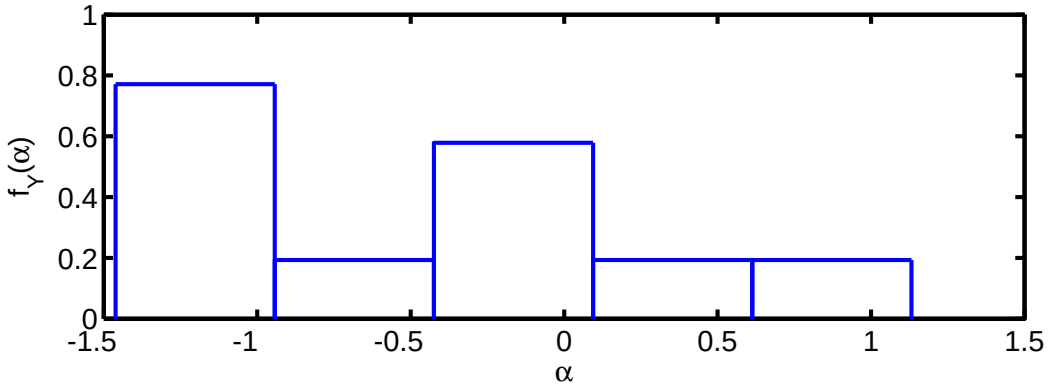

Figure D.3: Histogram of the data.

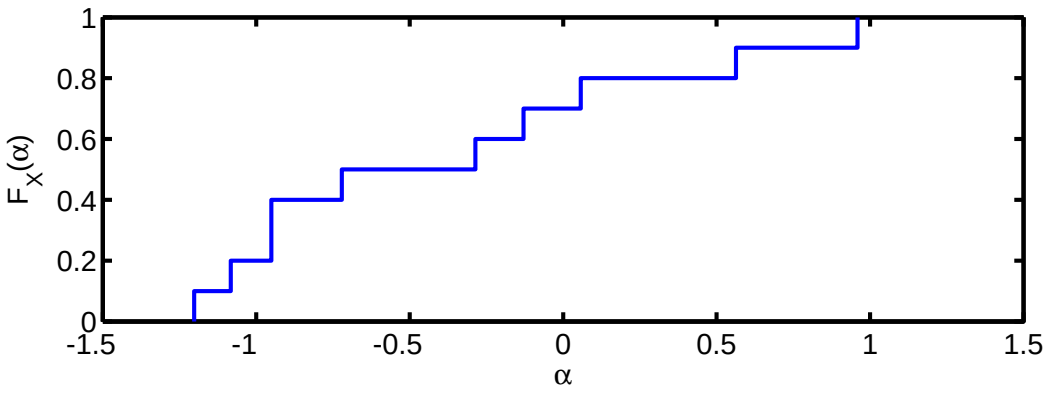

Figure D.4: Empirical CDF of the data.

The sample mean and sample standard deviation of the data are -0.374 and 0.737. The CDF of the Student's t-based sampling distribution of the mean is plotted (red) in Figure D.5. One-thousand bootstrap replicates of the sample mean were generated and analyzed as described above. The empirical CDF of bootstrap mean estimates – the sampling distribution for the mean – is shown Figure D.5 (blue). The CDFs match fairly closely; this is attributable to fact that the mean estimator is nearly normally distributed, even for an average based on ten data. The standard error for the mean estimate, based on the Student's t distribution is 0.264; the standard error for the mean estimate, based on the bootstrap analysis is 0.222. The symmetric, ninety percent confidence interval on the mean was obtained from the Student's t distribution; it is $[-0.801, 0.053]$ The limits of the interval are shown as red circles on red CDF curve. The ninety percent confidence interval on the mean was obtained from the bootstrap analysis; it is $[-0.723, 0.005]$. The limits of the interval are shown as blue circles on the blue CDF curve. In summary, the experimental bootstrap data reflect slightly lower variability than would be predicted using the Student's t distribution.

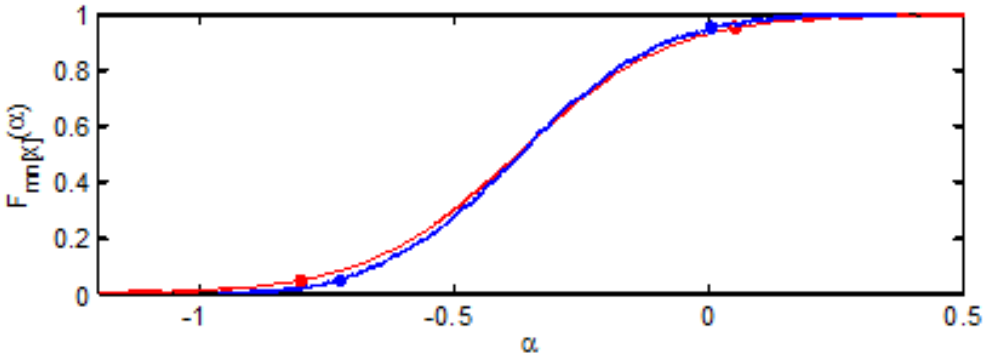

Figure D.5: PDF of the Student's t sampling distribution for the mean (red), and KDE of the sampling distribution for the mean (blue).

Example 2.Consider the ten data listed at the start of the previous example. In this example,

we estimate the fiftieth percentile of the random variable that is the source of the data, and then estimate the ninety percent confidence intervals of the estimate of the fiftieth percentile. The fiftieth percentile is the median of a probability distribution. When a random variable X has CDF $F_X(x)$, $-\infty < x < \infty$, then the median is defined:

$$x_{0.50} = F_X^{-1}(0.50) \tag{D.2}$$

When the random variable is continuous-valued the CDF is monotone increasing, therefore, it should be a direct matter to establish the percentage point anytime we have an estimate of $F_X(x)$ There is an asymptotic, normal approximation for the sampling distribution of the median when n, the number of data in the sample is large, but it may not be very accurate in the present case [7].

The computations performed here follow the bootstrap procedure and use the KDE to approximate some CDFs. We start by generating 2000 bootstrap samples of the data. The KDE of each bootstrap sample was computed, and then integrated to form the CDF of the sample. One hundred of the 2000 CDFs of bootstrap samples are shown in Figure D.6. Each CDF has a median that can be computed directly using Equation (a); each computed quantity is a bootstrap replicate of the sample median, and the collection is denoted $x_{0.50}^{(b)}, b = 1, \ldots, 2000$ The PDF of the bootstrap replicates of the median was estimated with the KDE, and that is shown in Figure D.7. That PDF reflects the sampling distribution of the median estimator. The symmetric, ninety percent confidence interval obtained from the KDE is indicated by blue circles. The interval is $[-0.826, 0.022]$. The normal, asymptotic approximation to the sampling distribution of the median was also computed and is shown by the red curve in Figure D.7. Its mean and variance are $\left(-0.504, (0.375)^2\right)$. The ninety percent confidence interval on the median obtained from the asymptotic approximation is $[-1.122, 0.112]$, and is indicated by red circles in Figure D.7. As in the previous example, the variability of the median estimator is over-estimated by the asymptotic approximation.

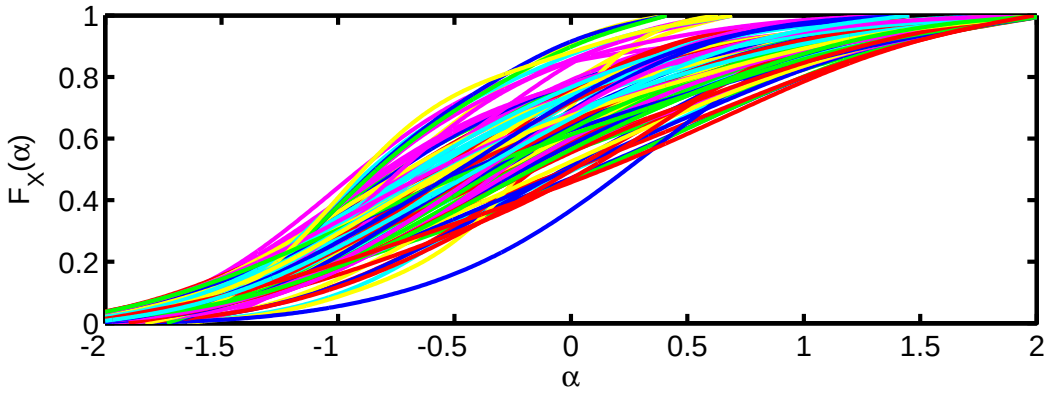

Figure D.6: One hundred (of the 2000 computed) KDE approximations to the CDFs of the bootstrap samples.

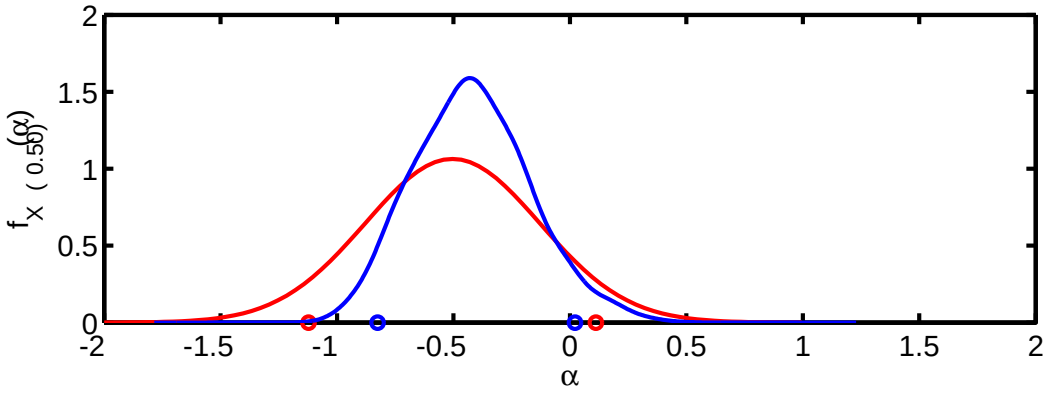

Figure D.7: KDE of the 2000 bootstrap replicates of the distribution median.

This page intentionally left blank.

Appendix E

Discussion of the Nonlinear Dynamic Example

This appendix details the non-linear structural mechanics example used throughout the report and in the validation analysis, a completely simulated or virtual example. The virtual structure under consideration is shown in Figure E.1. The analysis in this appendix explores response of the structure to random vibration, and uses "measured" responses of the Truth Model to calibrate the stochastic model for stiffness and damping. The Truth Model and the linear model are used in the body of the text to assess response of both structures to mechanical shock. For the purposes of validation and making conservative predictions, the linearized model is used to generate the model predictions. The linear model should be as close as possible to the Truth model. Because the Truth model is stochastic, the linear model must be stochastic as well; therefore part of the linearization scheme involves estimation of a PDF.

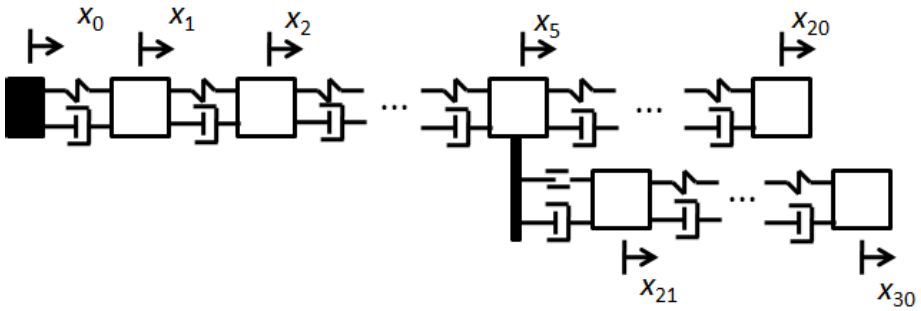

Figure E.1: Virtual structure to be analyzed

E.1 The non-linear (Truth) model

The structure to be analyzed is base-driven, has 30 discrete masses, and responds in one dimension. The quantities x_j, $j = 0, \ldots, 30$ denote absolute displacements of the base and the system masses; these also denote degrees-of-freedom (DOF) of the structure. The mass of the element

under x_0 is immaterial to the analysis; the mass is rigid and a motion is enforced at that location. The elements associated with the displacements x_j, $j = 1,\ldots,30$, have masses m_j, $j = 1,\ldots,30$. The connections between masses are modeled by a damper and a spring. For $j = 1,\ldots,30$, the damper to the left of DOF j has damping constant c_j and the spring to the left of DOF j (except for DOF 21) has stiffness k_j. The spring to the left of DOF 21 is nonlinear, and the restoring force in that spring is denoted $R(x_{21} - x_5)$. The element shown as a solid black bar that extends down from DOF 5 is a rigid, massless element. Masses one through twenty are given by the formula

$$m_j = 0.0045\,(20.5 - j/2) \quad \text{for} \quad j = 1,\ldots,20 \tag{E.1}$$

The structure, DOF 1-20, weighs 529.79 lbs. Stiffnesses one through twenty are given by the formula

$$k_j = 0.5 \times 10^4\,(20.5 - j/2) \quad \text{for} \quad j = 1,\ldots,20 \tag{E.2}$$

These quantities can be used to construct the 20×20 structure mass and stiffness matrices, $\mathbf{m}_0$ and $\mathbf{k}_0$. The structure damping matrix is defined as

$$\mathbf{c}_0 = \alpha_0 \mathbf{m}_0 + \beta_0 \mathbf{k}_0 \tag{E.3}$$

where $\alpha_0 = 4.5$ and $\beta_0 = 2.4 \times 10^{-5}$. This form of damping is Rayleigh damping.

Masses twenty-one through thirty are given by

$$m_{20+j} = \begin{cases} 0.062 & \text{for} \quad j = 1,2,3 \\ 0.6 \times 0.062 & \text{for} \quad j = 4,\ldots,7 \\ 0.4 \times 0.062 & \text{for} \quad j = 8,9,10 \end{cases} \tag{E.4}$$

The component, DOF 21-30, weighs 157.95 lbs. Stiffnesses twenty-two through thirty are given by

$$k_{21+j} = \begin{cases} 6.7 \times 10^4 & \text{for} \quad j = 1,2,3 \\ 0.8 \times 6.7 \times 10^4 & \text{for} \quad j = 4,5,6 \\ 0.6 \times 6.7 \times 10^4 & \text{for} \quad j = 7,8,9 \end{cases} \tag{E.5}$$

These quantities can be used to construct the 10×10 component mass and stiffness matrices, $\mathbf{m}_1$ and $\mathbf{k}_1$. (The component is free-in-space.) The component damping matrix is defined by

$$\mathbf{c}_1 = \alpha_1 \mathbf{m}_1 + \beta_1 \mathbf{k}_1 \tag{E.6}$$

where $\alpha_1 = 6$ and $\beta_1 = 1.3 \times 10^{-5}$.

The elastic spring element that connects DOF 5 and 21 exerts the restoring force defined by

$$R(z) = \begin{cases} k_{\text{lim}}\,(z + z_c) - R_c & \text{for} \quad z \le -z_c \\ a_1 z + a_3 z^3 & \text{for} \quad -z_c < z < z_c \\ k_{\text{lim}}\,(z - z_c) + R_c & \text{for} \quad z \ge z_c \end{cases} \tag{E.7}$$

The restoring force is meant to approximate the behavior of an ideal gap element. It does so by defining a limiting stiffness, k_{lim}, effective outside the interval $[-z_c, z_c]$, and a cubic restoring force within the interval $[-z_c, z_c]$. The cubic is defined to have stiffness at zero deformation of $0.1k_{\text{lim}}$, and slope of the restoring force at $\mp z_c$ that matches the limiting stiffness, k_{lim}. Denote by z_{gap} the width of the gap to be simulated. Then the parameters of Eq. (E.7) are defined as

$$a_1 = 0.1k_{\text{lim}} \quad \text{and} \quad z_c = 0.75z_{\text{gap}} \tag{E.8}$$

The parameters a_3 and z_c are computed iteratively. First, compute $a_3 = (k_{\text{lim}} - a_1) \Big/ \left(3z_c^2\right)$, and then $\varepsilon = -3a_3 z_{\text{gap}} z_c + 6a_3 z_c^2$. Modify z_c as long as ε is not near zero. When $\varepsilon \cong 0$, the iteration is complete. Finally,

$$R_c = a_1 z_c + a_3 z_c^3 \tag{E.9}$$

In the present model, k_{lim} and z_{gap} are normally distributed random variables with means and variances $\left(75 \times 10^3, \left(15 \times 10^3\right)^2\right)$ and $\left(0.005, (0.001)^2\right)$.

For example, when the nonlinear spring restoring force parameters are $k_{\text{lim}} = 8.11 \times 10^4$, $z_c = 0.0042$, $R_c = 137.77$, $a_1 = 8.11 \times 10^3$, and $a_3 = 1.35 \times 10^9$, the restoring force curve is the one shown in Figure E.2.

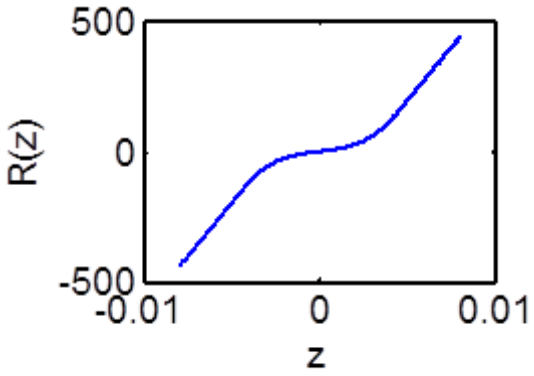

Figure E.2: Typical nonlinear restoring force curve

The equation governing base-excited motion is solved to obtain the response of the structure in Figure E.1. To write the equation we first define mass, damping and stiffness matrices for the entire structure.

$$\mathbf{m} = \begin{bmatrix} \mathbf{m}_0 & 0 \\ 0 & \mathbf{m}_1 \end{bmatrix} \mathbf{c} = \begin{bmatrix} \mathbf{c}_0 & 0 \\ 0 & \mathbf{c}_1 \end{bmatrix} \mathbf{k} = \begin{bmatrix} \mathbf{k}_0 & 0 \\ 0 & \mathbf{k}_1 \end{bmatrix} \tag{E.10}$$

where the mass, damping and stiffness matrices are the ones defined above, and the $\mathbf{0}$'s are appropriately sized matrices of zeros.

The equation of motion for the base-excited structure is

$$\mathbf{m}\ddot{\mathbf{z}} + \mathbf{c}\dot{\mathbf{z}} + \mathbf{k}\mathbf{z} + \mathbf{R}(\mathbf{z}) = -\mathbf{m}\,\mathbf{w}\,\ddot{x}_0 \qquad \mathbf{z}(0) = \mathbf{z}_0 \quad \dot{\mathbf{z}}(0) = \mathbf{v}_0 \tag{E.11}$$

with initial conditions provided to specify the response. The 30×1 vector $\mathbf{z} = \mathbf{x} - \mathbf{w}x_0$ contains the relative displacement responses at the structure DOF. The vector $\mathbf{w}$ is a 30×1 vector of ones. The scalar function $\ddot{x}_0$ is the enforced base acceleration. Dots denote differentiation with respect to time. The bold vector $\mathbf{R}(\mathbf{z})$ has dimension 30×1 and contains mostly zeros. The fifth and twenty-first elements, $R_5(z)$ and $R_{21}(z)$, in $\mathbf{R}(\mathbf{z})$ are non-zero, and given by

$$R_5(z) = -R(z_{21} - z_5) - c_{jt}(\dot{z}_{21} - \dot{z}_5) \quad \text{and} \quad R_{21}(z) = -R_5(z) \tag{E.12}$$

where $R(\bullet)$ is the function defined in Eq. E.7 and c_{jt} is a quantity drawn from a normally distributed random source with mean and variance $(1.5, (0.3)^2))$. Our definition of k_{lim}, z_{gap} and c_{jt} as random variables allows the structure to be random and captures the aleatory uncertainty in the properties of the non-linear joint.

The excitation to the structure is a realization from a wide-band, zero-mean, normal random process drawn from the source with spectral density shown in Figure E.3.

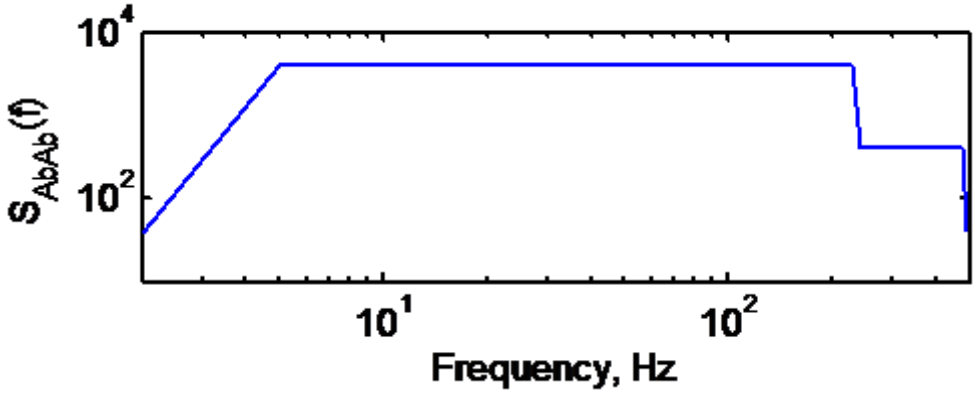

Figure E.3: Spectral density of acceleration of random excitations

The equations governing motion, Eq. (E.11), can be solved using several different approaches. We choose to solve them using the Runge-Kutta fourth order method. Relative motions between structure DOFs and the base motion are obtained. These can be used in $\ddot{\mathbf{x}}$=$\ddot{\mathbf{z}} + \mathbf{w}\ddot{x}_0$ to compute absolute measures of response.

E.2 Example: Random Vibration of the Truth Model

A segment of a base-excitation (acceleration) time history that comes from the specified random process is shown in Figure E.4. A segment of the total restoring force – nonlinear spring

restoring force plus linear viscous damper force – across the joint between DOFs 5 and 21 is shown in Figure E.5. A segment of the absolute acceleration on DOF 26 is shown in Figure E.6. A segment of the relative displacement across the joint from DOF 5 to DOF 21 is shown in Figure E.7. A segment of the relative velocity across the joint from DOF 5 to DOF 21 is shown in Figure E.8 Finally, a plot of the total restoring force across the joint that connects DOF 5 to DOF 21 as a function of relative displacement and relative velocity across the joint is shown in Figure E.9. (The view is along the relative velocity axis.) Because the nonlinear spring in the joint is elastic the restoring force curve would appear as a single curved line in the graph of Figure E.9 if the spring restoring force were plotted as a function of relative displacement across the joint. However, the graph reflects total restoring force viewed along the axis that is relative velocity across the joint. The total restoring force appears multi-valued at some points, because the velocity-related component of total restoring force differs depending on the sign of the relative velocity.

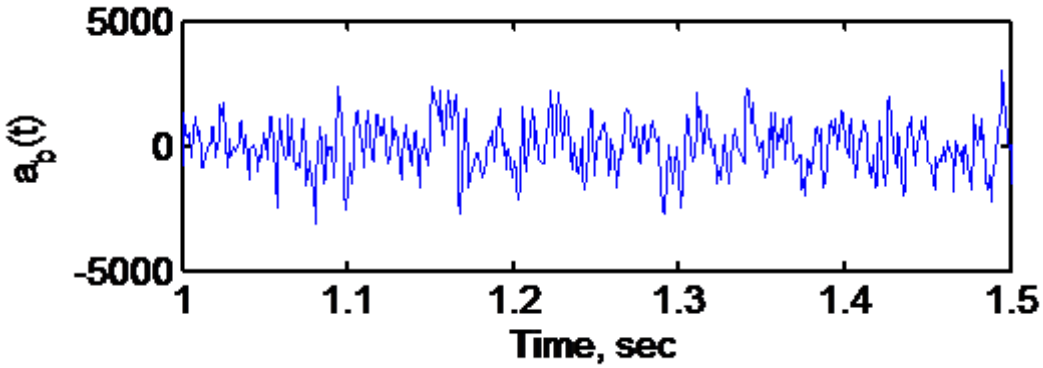

Figure E.4: Segment of acceleration applied to system using the Truth Model

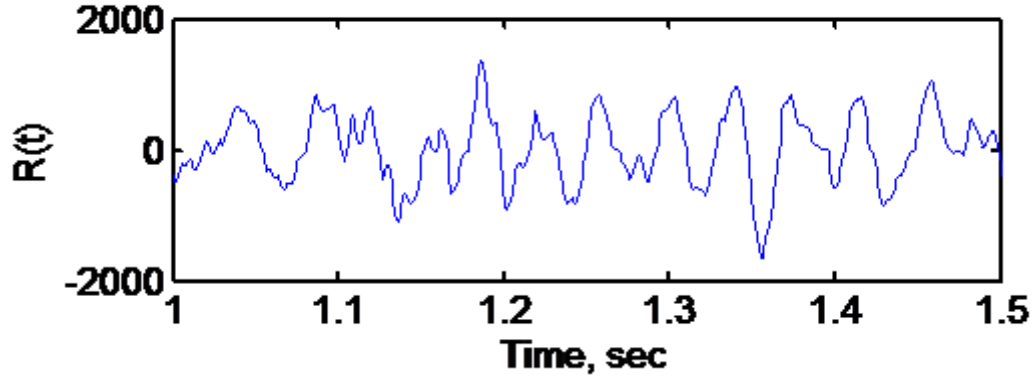

Figure E.5: Segment of total restoring force across joint DOF 5-21 (Truth Model)

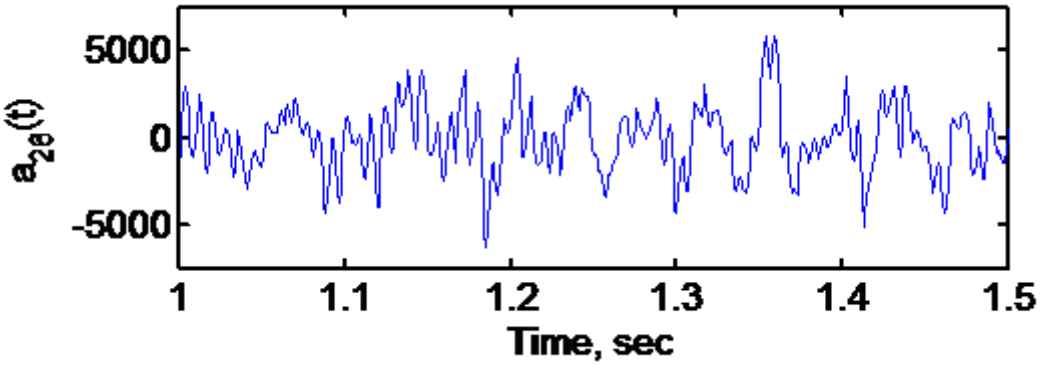

Figure E.6: Segment of absolute acceleration on DOF 26 (Truth Model)

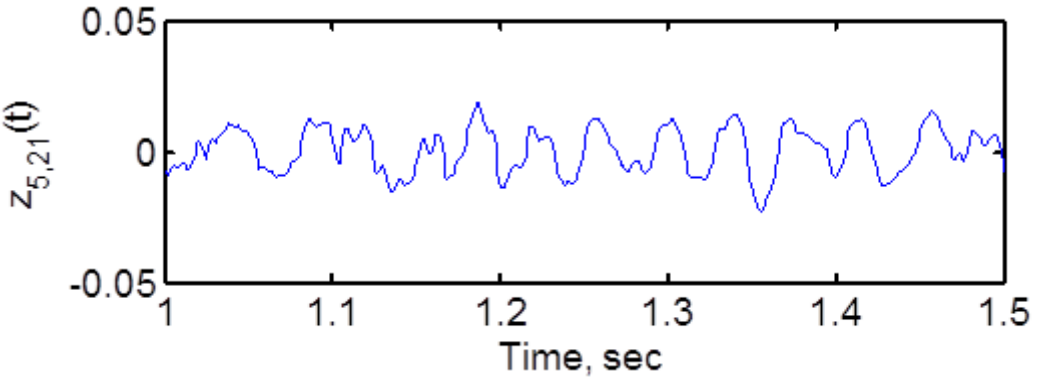

Figure E.7: Segment of relative displacement across joint between DOF 5-21 (Truth Model)

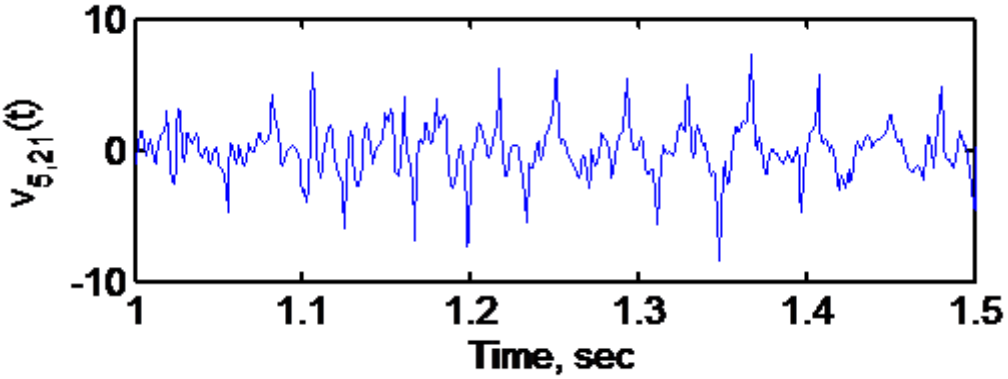

Figure E.8: Segment of relative velocity across joint between DOF 5-21 (Truth Model)

Twenty realizations of random process excitation like the one shown in Figure E.4 were generated and used to excite twenty separate, stochastic realizations of the Truth Model. For each realization we draw k_{lim}, z_{gap} and c_{jt} from their respective normal distributions. The nonlinear spring that joins DOF 5 to DOF 21 has the form of Eq. (E.7), and the spring parameters are random variable realizations as described following Eq. (E.9). The responses shown in Figure E.4 through Figure E.8 were recorded during each of the twenty response computations. All the computed responses have the same general character as the time histories shown in Figure E.4 through Figure E.8, though they differ in details. The twenty generated acceleration responses of the Truth Model at DOF 26 are shown in Figure E.10. The peaks of the absolute value of the acceleration responses at DOF 26 were observed, and the kernel density estimator (KDE, an approximation to the probability density function of a random variable) was computed. It is shown in Figure E.11.

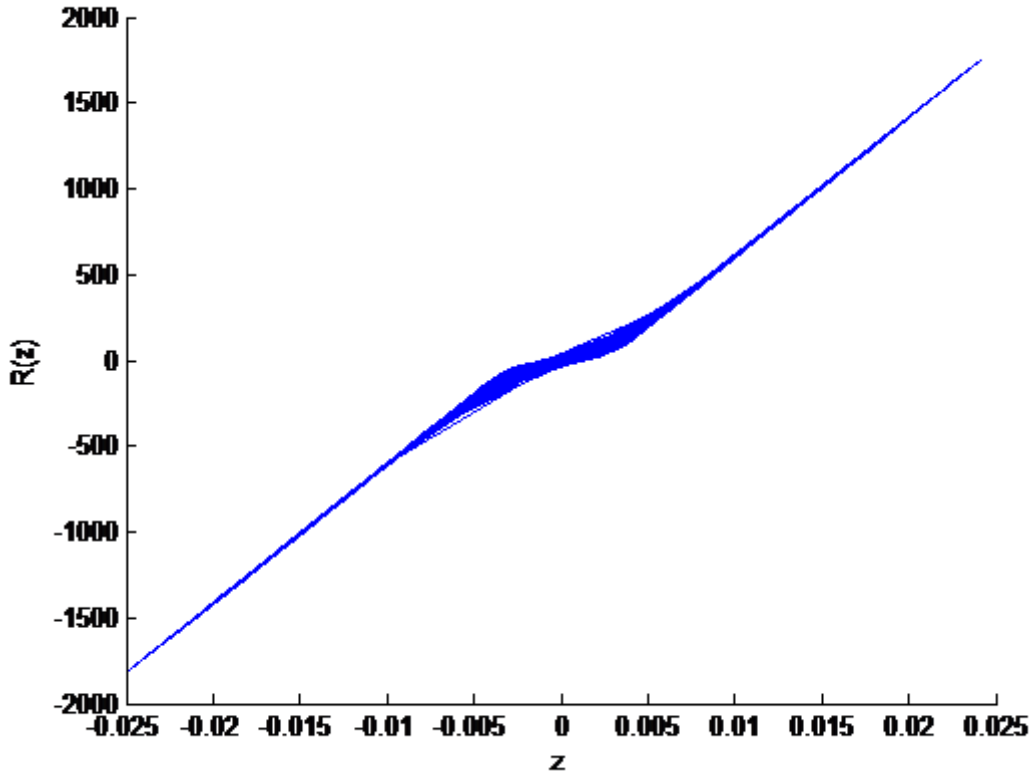

Figure E.9: Restoring force across joint that connects DOF 5-21 as function of relative displacement across joint, viewed along velocity axis (Truth Model).

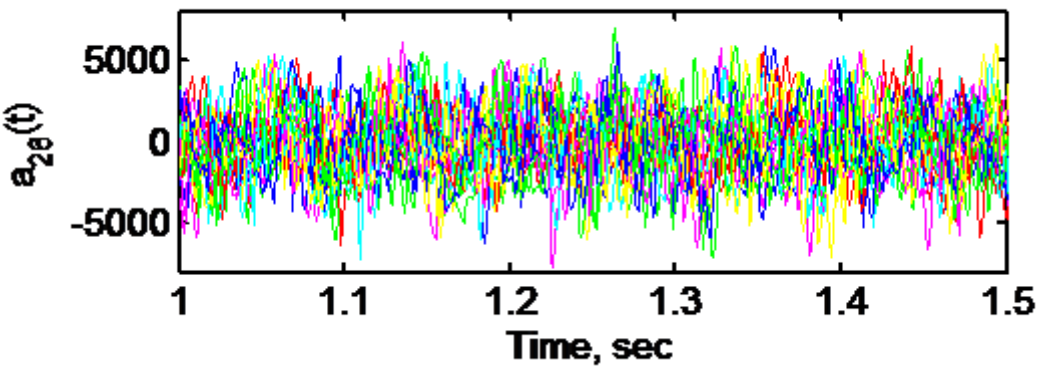

Figure E.10: Twenty acceleration responses at DOF 26. Excitations random and structures random. (Truth Model)

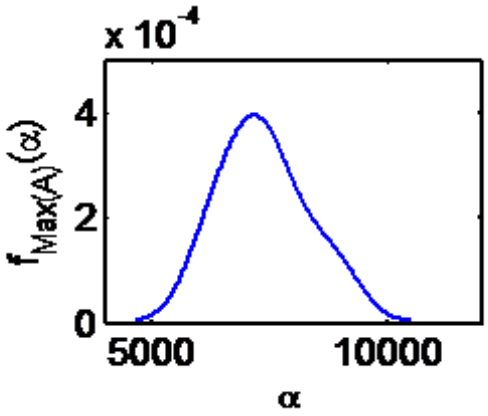

Figure E.11: Kernel density estimator of absolute peak acceleration responses at DOF 26. (Truth Model)

E.3 Linear Model

This section describes how we constructed a stochastic linear model of the Truth Model. In the validation section we consider how well the linear model predicts responses from the nonlinear Truth Model. There are several possible means for linearizing the Truth model while preserving the stochastic nature of the structure. A simple approach involves the following steps.

- Linearize the restoring force between DOF five and DOF twenty one for each realization of the stochastic Truth Model. The linear coefficients describe the equivalent, linearized mechanical joint stiffness and damping (k_{jt}, c_{jt}).
- Let (K_{jt}, C_{jt}) be jointly distributed random variables denoting mechanical joint stiffness and damping; we have twenty samples from this distribution. Estimate the PDF of the random source of the jointly distributed pairs with Karhunen-Loève expansion (KLE) with Markov Chain Monte Carlo (MCMC).

The operation described in the first bullet above was carried out on each set of the twenty input-response pairs from the Truth Model. The operation amounts to fitting the restoring force across the nonlinear joint with the linear expression $c_{jt}\dot{z} + k_{jt}z$

As specified in the second bullet above, we now form a KLE model of the random variable pair, (K_{jt}, C_{jt}). The model form is

$$\mathbf{Y} = \mathbf{V}\mathbf{W}^{1/2}\mathbf{U} + \mu_{\mathbf{Y}} \tag{E.13}$$

where $\mathbf{Y} = \left(K_{jt}, C_{jt}\right)^T$, $\mathbf{V}$ is the 2×2 matrix of eigen-vectors of the covariance matrix of $\mathbf{Y}$, $\mathbf{W}$ is the 2×2 diagonal matrix of eigenvalues (both positive when the covariance matrix is positive definite)

of the covariance matrix of $\mathbf{Y}$, $\mathbf{U}$ is a 2×1 vector of zero-mean, unit-variance, uncorrelated (but not necessarily independent) random variables, and $\mu_{\mathbf{Y}}$ is the 2×1 mean vector of $\mathbf{Y}$. The quantities $\mathbf{V}$, $\mathbf{W}$, and $\mu_{\mathbf{Y}}$, can be estimated using the measured data. Realizations of $\mathbf{U}$ that correspond to the realizations of $\mathbf{Y}$ can be computed by inverting Eq.(E.13). The bivariate KDE that approximates the bivariate probability density function (PDF) of $\mathbf{U}$ can be written. The MCMC approach can be used to sample the bivariate PDF of $\mathbf{U}$. Figure Figure E.12 illustrates this procedure. The blue dots are twenty linearized sets of coefficients (k_{jt}, c_{jt}). The red dots are twenty samples of stiffness and damping from the estimated KLE distribution.

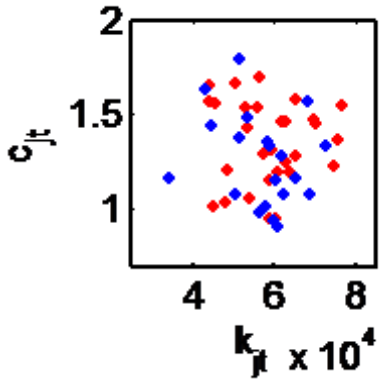

Figure E.12: Generated (red) and Truth-model-based (blue) pairs of equivalent stiffness and damping

E.4 Example: Linearization of the Truth Model

A linear model was constructed from each of the fifty bivariate pairs of stiffness and damping. The linear structure is governed by Eq. (E.11). As before, $\mathbf{R}(\mathbf{z})$ is a 30×1 vector containing mostly zeros, except for two terms. Those two terms are linear functions. Specifically,

$$r_5^i(z) = -k_{jt}^i(z_{21} - z_5) - c_{jt}^i(\dot{z}_{21} - \dot{z}_5) \tag{E.14}$$

$$r_{21}^i(z) = k_{jt}^i(z_{21} - z_5) + c_{jt}^i(\dot{z}_{21} - \dot{z}_5) \tag{E.15}$$

where $i = 1, \ldots, 50$ indexes the linear model and k_{jt}, c_{jt} are the linearized stiffness and damping. The same twenty excitations that were used to excite the Truth model as used as inputs to the fifty linear structure models in this way by choosing one at random. The same response values recorded during analysis of the Truth Model were also recorded during analysis of the linear model. For the sake of visual comparison to the Truth model, we present some of the same set of figures (E.5- E.8 for the linear model; Figure E.13 through Figure E.16 show one of the fifty computed response

measures. Figure E.13 shows a segment of the total restoring force across the joint between DOFs 5 and 21. Figure E.14 shows a segment of the absolute acceleration on DOF 26. Figure E.15 shows a segment of the relative displacement across the joint from DOF 5 to DOF 21. Figure E.16 shows a segment of the relative velocity across the joint from DOF 5 to DOF 21.

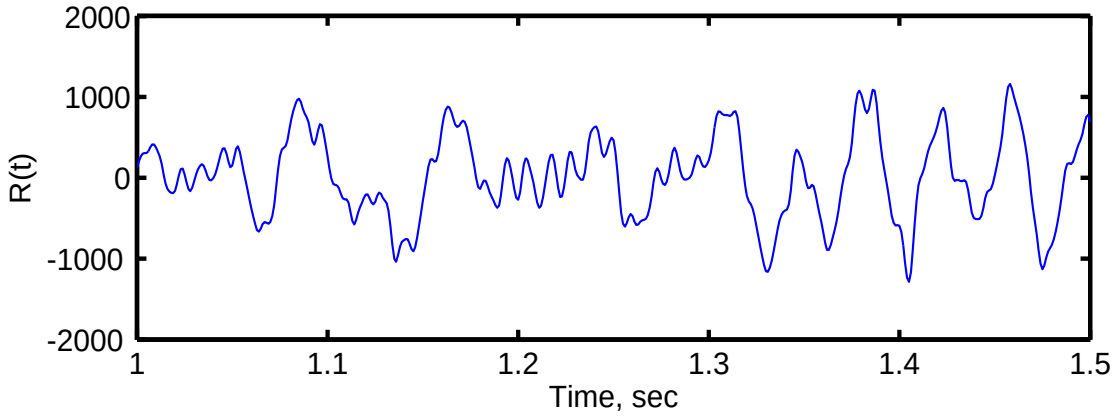

Figure E.13: Segment of total restoring force across joint from DOF 5-21 (linear model)

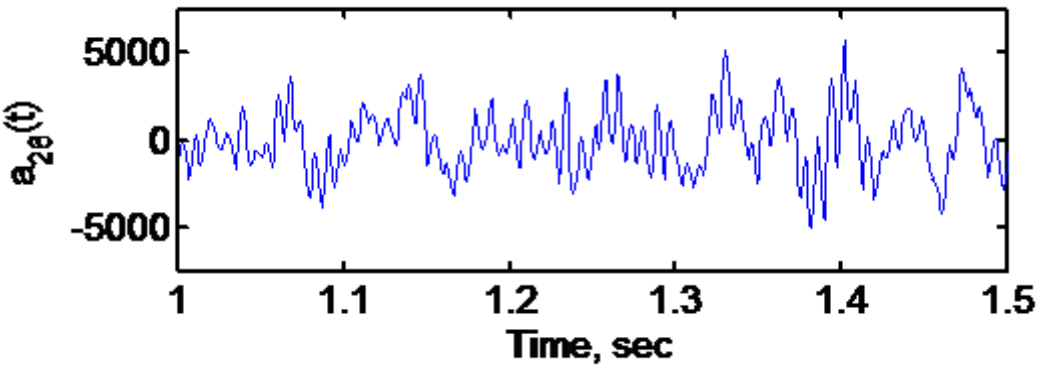

Figure E.14: Segment of absolute acceleration on DOF 26 (linear model)

Comparison of Figure E.15 to Figure E.7, relative displacement across the joint connecting DOF 5 to DOF 21 for the linear to nonlinear structures and Figure E.16 to Figure E.8, relative velocity across the joint for the linear to nonlinear structures indicates a relatively spiked character in the nonlinear structure response. This qualitative difference is often observed across hardening joints.

As mentioned, above, fifty linear model responses were computed. The entire collection of fifty absolute acceleration responses at DOF 26 is shown in Figure E.17. The peaks of the absolute value of the acceleration responses at DOF 26 were observed, and the KDE was computed. It is

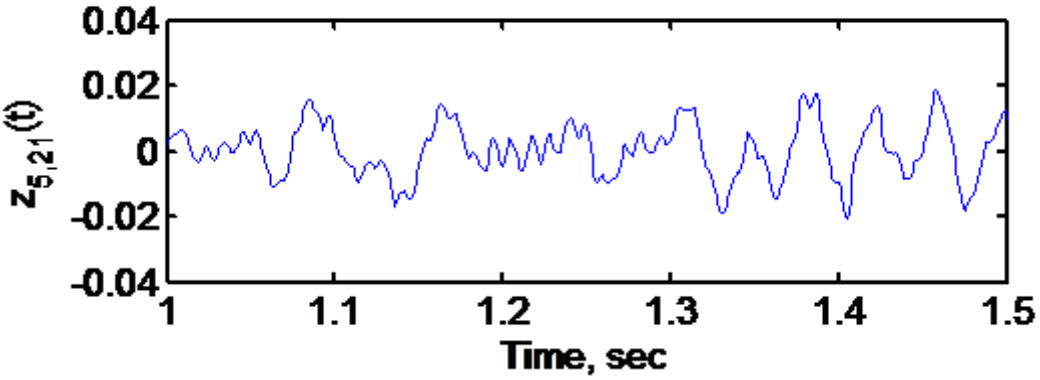

Figure E.15: Segment of relative displacement across joint between DOF 5-21 (linear model)

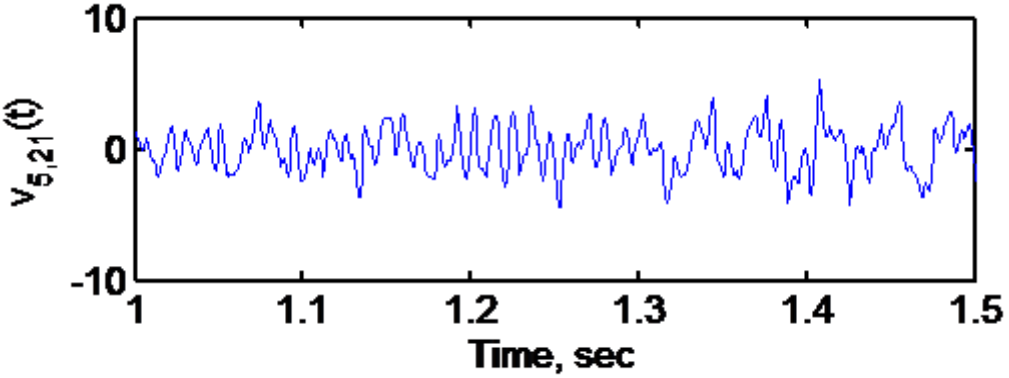

Figure E.16: Segment of relative velocity across joint between DOF 5-21 (linear model)

shown in Figure E.18 (red) along with the KDE from Figure E.11 (blue) indicating the estimated distribution of peaks at the same DOF in the nonlinear Truth Model. The results show what should be suspected, that is, that the joint in the nonlinear structure shows more high acceleration peaks at DOF 26. This tends to happen in hardening systems. The comparison shown in Figure E.18 can, by no means, form the basis for a validation comparison, because the parameters of the spring model used in the linear model were obtained from experiments that use the same inputs to both the Truth Model and the linear model. The responses of both structures to a different form of excitation needs to be obtained for a validation comparison to be performed. This is carried out in section 4.

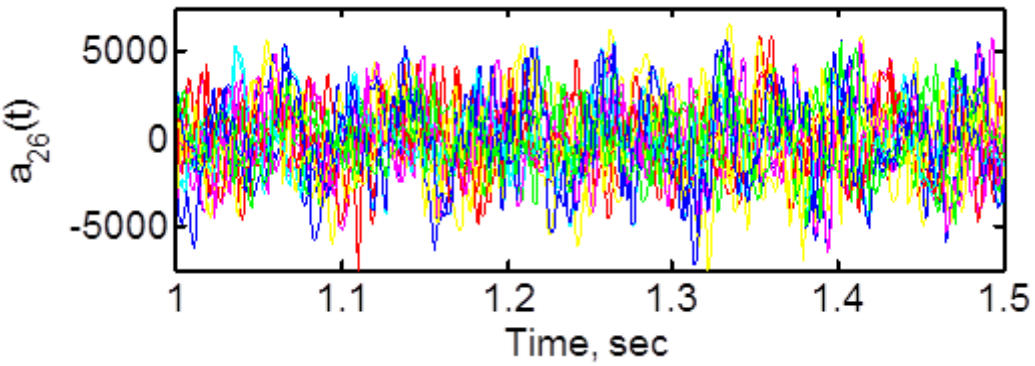

Figure E.17: Fifty acceleration responses in linear model at DOF 26

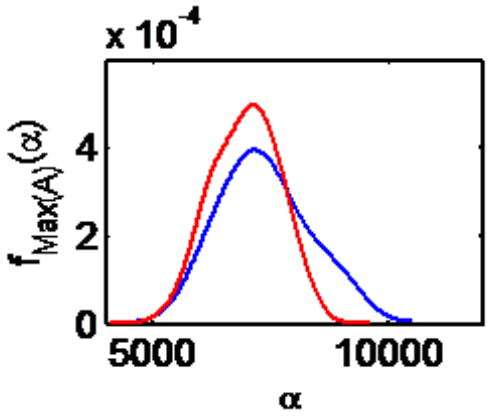

Figure E.18: Kernel density estimator of absolute peak acceleration responses in Truth Model (blue) and linear model (red)

DISTRIBUTION:

1 Professor Ron Averill
Department of Mechanical Engineering
Engineering Building
428 S. Shaw Lane, Room 2328-F
Michigan State University
East Lansing, MI 48824-1226
(Electronic Copy)

1 Charles R. Farrar
Los Alamos National Laboratory
P.O. Box 1663
Los Alamos, NM 8754
(Electronic Copy)

1 Francois M. Hemez
Los Alamos National Laboratory
P.O. Box 1663
Los Alamos, NM 8754
(Electronic Copy)

1 Professor Marc Mignolet
Arizona State University
Mechanical & Aerospace Engineering
P.O. Box 876106
Tempe, AZ 85287-6106
(Electronic Copy)

1 Prof. Kenneth Waldron
Department of Mechanical Engineering
Stanford University
Bldg. 520, Room 521Q
452 Escondido Mall
Stanford CA 94305-4021
(Electronic Copy)

1 Scott W. Doebling
Los Alamos National Laboratory
P.O. Box 1663
Los Alamos, NM 8754
(Electronic Copy)

1 Bob Ferencz
Lawrence Livermore National Laboratory
P.O. Box 808
Livermore, CA 94551
(Electronic Copy)

1 Shang-Rou (Henry) Hsieh
Lawrence Livermore National Laboratory
P.O. Box 808
Livermore, CA 94551
(Electronic Copy)

1 Peter J. Raboin
Lawrence Livermore National Laboratory
P.O. Box 808
Livermore, CA 94551
(Electronic Copy)

1	MS	0829	Newcomer, Justin T , 0431 (Electronic Copy)
1	MS	1318	Hendrickson, Bruce A. , 1440 (Electronic Copy)
1	MS	1318	Trucano, Timothy G. , 1440 (Electronic Copy)
1	MS	1318	Stewart, James R. & Org 01441 , (Electronic Copy)
1	MS	1323	Robinson, Allen C. , 1443 (Electronic Copy)
1	MS	0384	Johannes, Justine E. , 1500 (Electronic Copy)
1	MS	0828	Kempka, Steven N. , 1510 (Electronic Copy)
1	MS	828	Pilch, Martin & Org 01514 , (Electronic Copy)
1	MS	825	Payne, Jeffrey L. & Org 01515 , (Electronic Copy)
1	MS	840	Croessmann, Charles D. , 1520 (Electronic Copy)
1	MS	557	Jones, Darrick M. & Org 01521 , (Electronic Copy)
1	MS	557	Epp, David & Org 01522 , 1522 (Electronic Copy)
1	MS	557	Simmermacher, Todd W. & Org 01523 , (Electronic Copy)
1	MS	840	Fang, Huei Eliot & Org 1524 , (Electronic Copy)
1	MS	840	Pott, John & Org 1525 , (Electronic Copy)
1	MS	346	Peebles, Diane E. & Org 1526 , (Electronic Copy)
1	MS	386	Edwards, Timothy S. & Org 1527 , (Electronic Copy)
1	MS	828	Witkowski, Walter R. & Org 1544 , (Electronic Copy)
1	MS	9013	Lauffer, James P. , 8231 (Electronic Copy)
1	MS	9042	Gonzales, Mary E. , 8250 (Electronic Copy)
1	MS	9042	Moen, Christopher D. & Org 8256 , (Electronic Copy)
1	MS	9042	Chiesa, Michael L. & Org 8259 , (Electronic Copy)
1	MS	9158	Costa, James E. , 8950 (Electronic Copy)
1	MS	9159	McNeish, Jerry & Org 8954 , (Electronic Copy)
1	MS	0899	Technical Library, 8944 (electronic copy)

This page intentionally left blank.


Sandia National Laboratories